Received: 26 February 2021 | Accepted: 26 April 2021

DOI: 10.1002/asna.202113972

Astronomische Nachrichten

ORIGINAL ARTICLE

Gaia search for stellar companions of TESS Objects of Interest II

Markus Mugrauer | **Kai-Uwe Michel**

Astrophysikalisches Institut und Universitäts-Sternwarte Jena, Jena, Germany

Correspondence
M. Mugrauer, Astrophysikalisches Institut und Universitäts-Sternwarte Jena, Schillergäßchen 2, D-07745 Jena, Germany.
Email: markus@astro.uni-jena.de

Abstract

We present the latest results of our ongoing multiplicity study of (Community) TESS Objects of Interest, using astro- and photometric data from the ESA-Gaia mission, to detect stellar companions of these stars and to characterize their properties. In total, 107 binary, 5 hierarchical triple star systems, as well as one quadruple system were detected among 585 targets surveyed, which are all located at distances closer than about 500 pc around the Sun. As proven with their accurate Gaia EDR3 astrometry, the companions and the targets are located at the same distance and share a common proper motion, as it is expected for components of gravitationally bound stellar systems. The companions exhibit masses in the range between about 0.09 $M_{\odot}$ and 4.5 $M_{\odot}$ and are most frequently found in the mass range between 0.15 and 0.6 $M_{\odot}$. The companions are separated from the targets by about 120 up to 9,500 au and their frequency is the highest and constant within about 500 au while it continually decreases for larger separations. Beside mainly early to mid M dwarfs, also five white dwarf companions were identified in this survey, whose true nature was revealed by their photometric properties.

KEYWORDS

binaries: visual, white dwarfs, stars: individual (TOI2092B, TOI2127B, CTOI253040591B, CTOI341411516B, CTOI369376388C)

1 | INTRODUCTION

In 2020, we have initiated a new survey at the Astrophysical Institute and University Observatory Jena with the goal to explore the multiplicity of (Community) TESS Objects of Interest (CTOIs), i.e. stars, which are photometrically monitored by the Transiting Exoplanet Survey Satellite (TESS, Ricker et al. 2015) and exhibit promising dips in their light curves, that could be caused by potential exoplanets, which revolve around these stars.

In our survey stellar companions of (C)TOIs are detected and their properties are determined with astro- and photometry, originally taken from the 2nd data release (Gaia DR2 from hereon, Gaia Collaboration et al. 2018)

This research is based on observations made with the NASA/ESA Hubble Space Telescope, obtained from the Space Telescope Science Institute, which is operated by the Association of Universities for Research in Astronomy, under NASA contract NAS 5–26555. These observations are associated with the program 14260.

of the ESA-Gaia mission. The first results of the survey were presented by Mugrauer & Michel (2020), who have already explored the multiplicity of about 1,400 (C)TOIs, which were all listed in the (C)TOI release of the `Exoplanet Follow-up Observing Program` for TESS (ExoFOP-TESS)[1] by the end of May 2020. In the meantime, several of these (C)TOIs, which were revealed as members of multiple star systems in the course of our survey, could already be confirmed by follow-up observations to be exoplanet host stars, e.g. TOI 451, 1098, 1259, and 1333 (Martin et al. 2021; Newton et al. 2021; Rodriguez et al. 2021; Tofflemire et al. 2021).

Due to the successful execution of the TESS mission and the photometric analysis of its data the number of (C)TOIs and hence the number of targets of our survey is continuously growing. Since the end of May 2020 many hundreds of new (C)TOIs have been announced by the ExoFOP-TESS and we could already investigate the multiplicity of these stars, which is presented in this paper.

In the following section, we describe in detail the properties of the selected targets, as well as the search for companions around these stars. In Section 3, we present all (C)TOIs with detected companions and characterize the properties of these stellar systems. A summary of the current status of our survey and an outlook for the project are given in the last section of this paper.

2 | SEARCH FOR STELLAR COMPANIONS OF (C)TOIS BY EXPLORING THE GAIA EDR3

In contrast to Mugrauer & Michel (2020), the search for companions, presented here, uses astro- and photometric data from the early version of the 3rd data release (Gaia EDR3 from hereon, Gaia Collaboration et al. 2020) of the ESA-Gaia mission, which was just recently published on December 3, 2020. The Gaia EDR3 is based on data, which could be collected with the instruments of the ESA-Gaia satellite during the first 34 months of its mission. This data release contains astrometric solutions, i.e. positions (α, δ), parallaxes π, and proper motions ($\mu_\alpha cos(\delta)$, μ_δ) of about 1.5 billion sources down to a limiting magnitude of 21 mag in the G-band, i.e. white light observations, taking advantage of the full spectral response of the utilized CCD-detectors. Parallaxes are determined with an uncertainty in the range of about 0.02 milliarcsec (mas) for bright ($G < 15$ mag, with a lower magnitude limit of $G \sim 1.7$ mag) up to 0.5 mas for faint (G = 20 mag) detected sources. Proper motions are measured with an uncertainty of about 0.02 mas year^{-1} for bright objects, which increases up to 0.6 mas year^{-1} at G = 20 mag. In addition, for all sources their G-band magnitude is given with a photometric precision in the range between about 0.3 millimagnitude (mmag) for the brightest and 6 mmag for faint sources.

In the survey, presented here, stellar companions of the investigated (C)TOIs are identified at first as sources, which are located at the same distances as the targets, and secondly share a common proper motion with these stars. In order to clearly detect co-moving companions and prove their equidistance with the (C)TOIs, only sources are taken into account in this survey, which are listed in the Gaia EDR3 and exhibit significant measurements of their parallaxes ($\pi/\sigma(\pi) > 3$) and proper motions ($\mu/\sigma(\mu) > 3$). Thereby sources with a negative parallax are neglected.

As this survey was originally based on data of the Gaia DR2, which exhibits a typical parallax uncertainty of 0.7 mas for faint sources down to G = 20 mag, the survey is constrained to (C)TOIs within 500 pc around the Sun (i.e. $\pi > 2$ mas), to assure $\pi/\sigma(\pi) > 3$ even for the faintest detectable companions. This distance constraint is slightly relaxed to $\pi + 3\sigma(\pi) > 2$ mas, i.e. taking into account also the parallax uncertainty of the (C)TOIs. Although from now on data from the Gaia EDR3 are used, which has smaller parallax uncertainties, we will keep for the survey the chosen distance constraint for continuity reasons.

Between the end of May and the beginning of December 2020, in total 585 stars were added to the (C)TOI release of the ExoFOP-TESS, which fulfill this distance constraint, and therefore were selected as new targets of our survey. The target selection did not take into account (C)TOIs with dips in their light curves, which could already be classified as false positive detections by follow-up observations, carried out in the course of the ExoFOP-TESS. Furthermore, (C)TOIs which are confirmed exoplanet host stars, whose multiplicity was already studied with Gaia data by Mugrauer (2019) or Michel & Mugrauer (2021), were excluded as targets as well.

The histograms of the properties of all selected targets are summarized in Figure 1. The distances (*dist*) and the total proper motions (μ) of the targets were derived with their accurate Gaia EDR3 parallaxes (*dist*[pc] = 1000/π[mas]) and proper motions in right ascension and declination. The G-band magnitudes of all targets were taken from the Gaia EDR3, their masses and effective temperatures (T_{eff}) from the Starhorse Catalog (SHC from hereon, Anders et al. 2019), respectively.

The targets are located at distances between about 10 and 550 pc and exhibit proper motions in the range between about 1 and 1,650 mas year^{-1}, G-band magnitudes from 4.7 to 17 mag, effective temperatures from about

[1] Online available at: https://exofop.ipac.caltech.edu/tess/view_toi.php https://exofop.ipac.caltech.edu/tess/view_ctoi.php

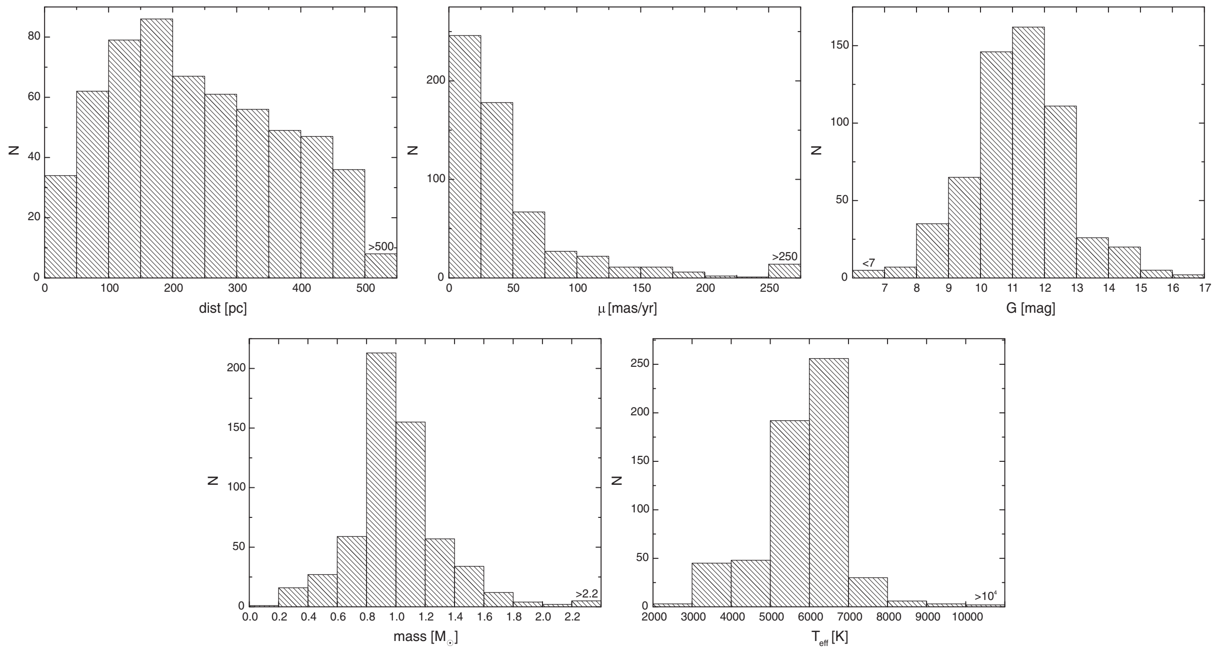

FIGURE 1 The histograms of the individual properties of all targets

2,900 up to 14,200 K, and masses, which range between about 0.2 and 4.8 $M_\odot$.

According to the cumulative distribution functions of the individual properties, the targets are most frequently located at distances between about 100 and 250 pc and have proper motions in the range between about 10 and 30 mas year^{-1}, as well as G-band magnitudes from $G = 10$ to 13 mag. The targets are mainly solar like stars with masses in the range between 0.9 and 1.2 $M_\odot$. This population also emerges in the $T_{\rm eff}$ distribution of the targets at intermediate temperatures of about 5,900 and 6,400 K. In addition, another but fainter pile-up of targets is evident in this distribution at lower effective temperatures between about 3,000 and 4,900 K, which is the early K to mid M dwarf population.

As defined and described in Mugrauer & Michel (2020) our survey is limited to companions with projected separations up to 10,000 au, which guarantees an effective companion search on one side but also detects the vast majority of all wide companions of the selected targets. This results in an angular search radius for companions around the targets of $r[\text{arcsec}] = 10\pi[\text{mas}]$, with π the Gaia EDR3 parallaxes of the (C)TOIs.

All sources, listed in the Gaia EDR3, which are located within the used search radius around the targets and exhibit significant parallaxes and proper motions are considered as companion-candidates. In total, 36,132 such objects were detected around 518 targets, investigated in the course of this survey. The companionship of all these candidates was tested based on their accurate Gaia EDR3 astrometry and that of the associated (C)TOIs, exactly following the procedure, as described in Mugrauer & Michel (2020). The vast majority of these sources (>99.7%) could be excluded as companions, as they do not share a common proper motion with the (C)TOIs and/or are not located at the same distances as these stars. In contrast, for 119 candidates the companionship to the (C)TOIs could clearly be proven with their accurate Gaia EDR3 astrometry. The properties of these companions and of the associated (C)TOIs are described in detail in the next section of this paper.

3 | (C)TOIS AND THEIR DETECTED STELLAR COMPANIONS

The masses, effective temperatures, and absolute G-band magnitudes of the (C)TOIs with detected companions, presented here, are all listed in the SHC and we plot these stars in the $T_{\rm eff} - M_{\rm G}$ diagram, which is shown in Figure 2. For comparison, we plot in this diagram the main sequence from Pecaut & Mamajek (2013).[2]

The vast majority of all targets with detected companions are main-sequence stars. Few (C)TOIs are located (significantly) above the main sequence and all of these stars exhibit surface gravities $\log(g[\text{cm/s}^{-2}]) \lesssim 3.8$, as listed in the SHC, hence they are classified as (sub)giants.

The parallaxes, proper motions, apparent G-band magnitudes, and extinction estimates of the (C)TOIs and their

[2]Online available at: http://www.pas.rochester.edu/~emamajek/EEM_dwarf_UBVIJHK_colors_Teff.txt

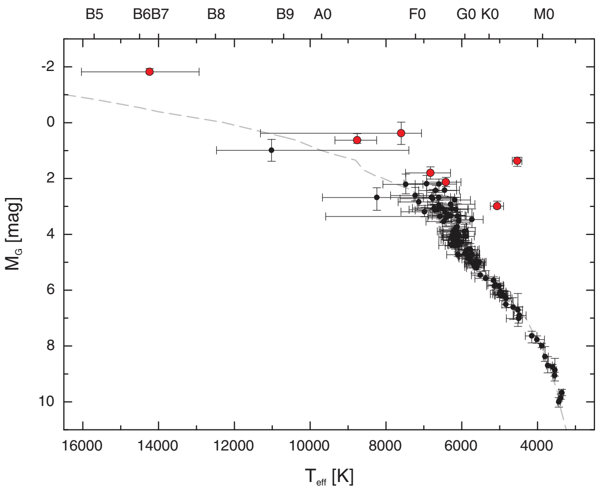

FIGURE 2 The $T_{\rm eff}$-$M_{\rm G}$ diagram of all (C)TOIs with detected companions, presented here. The main sequence is shown as gray dashed line. (C)TOIs, listed in the SHC with surface gravities $\log(g[{\rm cm/s^{-2}}]) \lesssim 3.8$, are illustrated as red circles, those with larger surface gravities with black circles, respectively

companions, detected in this survey, are summarized in Table 1, which lists in total, 107 binary, and 5 hierarchical triple star systems. In the case of CTOI 105850602 (alias HD 146759), which is shown in Figure 3, beside its close binary companion CTOI 105850602 CD, located at an angular separation of about 29 arcsec (~3,600 au of projected separation), whose two components are resolved by Gaia, the star also exhibits a close companion-candidate ($\rho \sim 0.3$ arcsec), whose relative astrometry is listed for two observing epochs in the Washington Double Star Catalog (WDS from hereon, Mason et al. 2001). The companion was observed in 2008 at $\rho = 0.3$ arcsec & $PA = 136°$, and in 2014 at $\rho = 0.3$ arcsec & $PA = 132°$, respectively. Adopting that this candidate is a non-moving background star, in 2014 we would have expected the object to be located at $\rho = 0.35$ arcsec & $PA = 96.4°$, based on its 1st epoch astrometry and the accurate Gaia EDR3 parallax and proper motion of the CTOI. Because the companion exhibits a constant angular separation in both observing epochs and in particular its position angle does not decrease by about 40° between both observing epochs, as expected for a non-moving background source, we conclude that this candidate is a co-moving companion of CTOI 105850602. Therefore, this CTOI is actually the primary component of a stellar quadruple system.

For all detected companions, we determined their angular separation (ρ) and position angle (PA) to the associated (C)TOIs, using the accurate Gaia EDR3 astrometry of the individual objects. The obtained relative astrometry of the companions is listed in Table 2, together with its uncertainty, which remains below about 1 mas in angular separation, and 0.03° in position angle, respectively.

The parallax difference $\Delta\pi$ between the (C)TOIs and their companions together with its significance sig-$\Delta\pi$ was calculated (in addition also by taking into account the astrometric excess noise of the individual objects) and is summarized in Table 2. In the same table for each companion, its differential proper motion $\mu_{\rm rel}$ relative to the associated (C)TOI is listed with its significance, as well as its *cpm-index*.[3]

The parallaxes of the individual components of the stellar systems, presented here, do not significantly differ from each other (sig-$\Delta\pi < 3$), when the astrometric excess noise is taken into account. This clearly proves the equidistance of the detected companions with the (C)TOIs, as expected for components of physically associated stellar systems. Furthermore, the vast majority of the detected companions (more than 96% of all) exhibit a *cpm-index* > 10 and all companions reach a *cpm-index* > 5. Hence, the detected companions and the associated (C)TOIs clearly form common proper motion pairs, as expected for gravitationally bound stellar systems.

The equatorial coordinates, as well as the derived absolute G-band magnitudes, projected separations, masses, and effective temperatures of all detected companions are summarized in Table 3.

The absolute G-band magnitudes of the companions are taken from the SHC if available, or were derived with their apparent G-band photometry and the parallaxes of the (C)TOIs from the Gaia EDR3, as well as the Apsis-Priam G-band extinction estimates, listed in the Gaia DR2. Thereby, always the extinction estimates of the companions if available, otherwise those of the (C)TOIs were used. For systems with no G-band extinction estimates, listed for any of their components, we have used the extinction estimates of the (C)TOIs from the SHC if available or from the Starhorse catalog for five surveys (Queiroz et al. 2020), indicated with the `SHC` and `SHC5` flag in Table 1, respectively. Thereby, V-band extinctions given in these catalogues were transformed to the G-band using the relation $A_{\rm G}/A_{\rm V} = 0.77$, as determined by Mugrauer (2019).

The projected separations of all companions were derived from their angular separations to the associated (C)TOIs and the parallaxes of these stars.

The masses and effective temperatures of all detected companions, presented here, including their uncertainties, are taken from the SHC if available, which applies to about 70% of all companions. In Figure 4, we plot these companions in a $T_{\rm eff}$-$M_{\rm G}$ diagram, together with the companions for which Apsis-Priam estimates of their effective

[3]The degree of common proper motion of a detected companion with the associated (C)TOI is characterized by its common proper motion (cpm) index, as defined in Mugrauer & Michel (2020).

TABLE 1 This table summarizes for all (C)TOIs (listed at first) and their detected companions their Gaia EDR3 parallaxes π, proper motions μ in right ascension and declination, astrometric excess noises *epsi*, G-band magnitudes, as well as the used Apsis-Priam G-band extinction estimates A_G or if not available the G-band extinctions, as listed either in the SHC or in the SHC5, indicated with SHC and SHC5, respectively

TOI	π (mas)	$\mu_\alpha cos(\delta)$ (mas year^{-1})	μ_δ (mas year^{-1})	*epsi* (mas)	*G* (mag)	A_G (mag)	
1937 A	2.4113 ± 0.0108	-5.627 ± 0.013	11.309 ± 0.013	0.027	13.0048 ± 0.0028	$0.3990^{+0.2310}_{-0.1630}$	
1937 B	2.3514 ± 0.0891	-5.387 ± 0.104	11.349 ± 0.096	0.373	17.6530 ± 0.0034		
1940 A	3.7497 ± 0.0177	4.967 ± 0.021	-2.265 ± 0.016	0.097	9.8591 ± 0.0028	$0.3259^{+0.2092}_{-0.2092}$	SHC
1940 B	2.9986 ± 0.1211	4.181 ± 0.152	-0.663 ± 0.161	0.712	13.0511 ± 0.0045		
1943 A	7.6634 ± 0.0125	-91.364 ± 0.012	-24.450 ± 0.014	0.025	10.6662 ± 0.0028	$0.2485^{+0.0889}_{-0.1046}$	
1943 B	7.5589 ± 0.0458	-92.307 ± 0.045	-24.881 ± 0.057	0.397	14.6400 ± 0.0031		
1946 A	3.9857 ± 0.1243	-32.551 ± 0.126	-20.338 ± 0.124	0.918	8.7606 ± 0.0028	$0.1566^{+0.2006}_{-0.1566}$	SHC
1946 B	3.3840 ± 0.1615	-26.909 ± 0.176	-20.078 ± 0.132	0.952	12.7681 ± 0.0034		
1953 A	3.7995 ± 0.0314	-6.971 ± 0.036	-3.961 ± 0.031	0.223	9.8517 ± 0.0028	$1.2685^{+0.0835}_{-0.1765}$	
1953 B	3.8352 ± 0.1079	-7.352 ± 0.133	-3.312 ± 0.107	0.311	17.5745 ± 0.0033		
1964 A	2.5086 ± 0.0198	-19.280 ± 0.022	3.241 ± 0.016	0.136	11.1381 ± 0.0028	$0.0105^{+0.1119}_{-0.0105}$	SHC
1964 B	2.4861 ± 0.0628	-19.105 ± 0.066	3.314 ± 0.057	0.237	16.5546 ± 0.0036		
1966 A	3.7310 ± 0.0380	-39.460 ± 0.037	1.372 ± 0.046	0.285	9.3827 ± 0.0028		
1966 B	3.3062 ± 0.0196	-38.402 ± 0.020	1.287 ± 0.025	0.000	14.0628 ± 0.0028	$0.7567^{+0.1699}_{-0.2802}$	
1970 A	2.4254 ± 0.0365	-19.008 ± 0.029	-0.431 ± 0.028	0.317	11.3380 ± 0.0028	$0.8230^{+0.2910}_{-0.2274}$	
1970 B	2.4923 ± 0.0828	-19.215 ± 0.066	-0.414 ± 0.070	0.000	17.3905 ± 0.0029		
1972 A	5.0597 ± 0.0123	-9.982 ± 0.013	34.161 ± 0.014	0.056	10.1464 ± 0.0028		
1972 B	5.0479 ± 0.0115	-9.781 ± 0.013	33.776 ± 0.013	0.050	10.6799 ± 0.0028	$0.0780^{+0.2566}_{-0.0610}$	
1984 A	4.0450 ± 0.0135	-12.779 ± 0.010	-24.344 ± 0.011	0.083	10.7127 ± 0.0028	$0.0260^{+0.1245}_{-0.0260}$	
1984 B	4.0759 ± 0.2280	-12.242 ± 0.172	-24.758 ± 0.172	0.905	18.1146 ± 0.0081		
1992 A	2.6006 ± 0.0153	0.481 ± 0.012	-7.645 ± 0.014	0.099	10.8569 ± 0.0028		
1992 B	2.6098 ± 0.0234	0.092 ± 0.020	-7.758 ± 0.022	0.204	11.3123 ± 0.0028	$0.4967^{+0.2533}_{-0.3633}$	
2001 A	2.2236 ± 0.0196	-2.694 ± 0.024	2.659 ± 0.024	0.185	9.1756 ± 0.0028	$0.3032^{+0.3928}_{-0.3032}$	SHC
2001 B	2.4396 ± 0.0925	-3.651 ± 0.108	3.820 ± 0.227	0.649			
2006 A	2.0109 ± 0.0117	8.281 ± 0.015	22.092 ± 0.013	0.045	9.9077 ± 0.0028		
2006 B	1.9621 ± 0.0159	7.662 ± 0.017	22.363 ± 0.019	0.079	13.1132 ± 0.0028	$0.4653^{+0.1268}_{-0.1830}$	
2009 A	48.6807 ± 0.0323	103.168 ± 0.036	-490.281 ± 0.025	0.161	8.0339 ± 0.0028		
2009 B	48.7040 ± 0.0478	96.607 ± 0.049	-495.495 ± 0.035	0.315	12.6158 ± 0.0028	$0.3915^{+0.1630}_{-0.1796}$	
2033 A	3.5400 ± 0.0118	24.900 ± 0.010	-2.831 ± 0.012	0.054	9.7429 ± 0.0028		
2033 B	3.5679 ± 0.0118	24.779 ± 0.010	-2.912 ± 0.012	0.062	10.6656 ± 0.0028	$0.6020^{+0.3616}_{-0.3314}$	
2036 A	4.4161 ± 0.0173	-17.432 ± 0.014	15.230 ± 0.013	0.121	9.3132 ± 0.0028	$1.1860^{+0.2960}_{-0.4734}$	
2036 B	4.3064 ± 0.0662	-16.975 ± 0.063	14.628 ± 0.060	0.336	16.3031 ± 0.0042		
2050 A	8.7474 ± 0.0114	20.878 ± 0.013	2.096 ± 0.013	0.086	10.1196 ± 0.0028		
2050 B	8.6148 ± 0.0366	23.547 ± 0.042	6.240 ± 0.039	0.403	13.6954 ± 0.0028	$0.3630^{+0.2810}_{-0.1361}$	
2056 A	10.7827 ± 0.0191	-98.730 ± 0.017	-9.845 ± 0.019	0.139	7.6570 ± 0.0028	$0.1313^{+0.1649}_{-0.1313}$	SHC

TABLE 1 Continued

TOI	π (mas)	$\mu_\alpha cos(\delta)$ (mas year^{-1})	μ_δ (mas year^{-1})	*epsi* (mas)	*G* (mag)	A_G (mag)	
2056 B	10.7935 ± 0.0175	-96.775 ± 0.016	-10.659 ± 0.018	0.147	12.3521 ± 0.0030		
2068 A	18.8696 ± 0.0131	-197.943 ± 0.013	-6.062 ± 0.013	0.097	12.2109 ± 0.0028		
2068 B	18.8558 ± 0.0144	-200.442 ± 0.015	-7.292 ± 0.015	0.116	12.4366 ± 0.0028	$0.3745^{+0.3516}_{-0.1616}$	
2072 A	25.6289 ± 0.0192	-184.967 ± 0.022	-87.241 ± 0.023	0.169	12.6971 ± 0.0028		
2072 B	25.5547 ± 0.0192	-184.594 ± 0.021	-92.030 ± 0.023	0.143	13.6121 ± 0.0028	$0.1350^{+0.1140}_{-0.1014}$	
2084 A	8.7499 ± 0.0166	47.731 ± 0.018	36.756 ± 0.019	0.000	14.3890 ± 0.0028	$0.0210^{+0.1170}_{-0.0140}$	
2084 B	8.7935 ± 0.7475	49.097 ± 0.825	38.893 ± 0.967	1.419	20.6793 ± 0.0093		
2092 A	5.6461 ± 0.0133	96.066 ± 0.011	-29.136 ± 0.014	0.110	11.0975 ± 0.0028	$0.1137^{+0.0977}_{-0.0718}$	
2092 B	4.1900 ± 0.7059	96.657 ± 0.693	-30.618 ± 0.776	1.273	19.4080 ± 0.0092		
2094 A	19.9111 ± 0.0129	-55.300 ± 0.016	-0.125 ± 0.017	0.072	13.4332 ± 0.0028	$0.3315^{+0.1336}_{-0.0416}$	
2094 B	20.0622 ± 0.1183	-54.380 ± 0.154	1.269 ± 0.150	0.896	18.0302 ± 0.0033		
2106 A	8.3310 ± 0.0136	-28.444 ± 0.011	-63.918 ± 0.013	0.103	10.3233 ± 0.0028	$0.1190^{+0.0940}_{-0.0930}$	
2106 B	8.4985 ± 0.4626	-25.845 ± 0.384	-60.689 ± 0.403	4.903	14.2890 ± 0.0047		
2108 A	3.9652 ± 0.0149	-0.348 ± 0.013	7.484 ± 0.014	0.106	10.5998 ± 0.0028	$0.4700^{+0.4091}_{-0.2686}$	
2108 B	3.9693 ± 0.0541	-0.694 ± 0.110	8.224 ± 0.046	0.330	12.8030 ± 0.0034		
2113 A	3.9296 ± 0.0172	-2.477 ± 0.020	-63.678 ± 0.025	0.182	10.9145 ± 0.0028		
2113 B	3.9522 ± 0.0240	-2.283 ± 0.027	-62.231 ± 0.036	0.255	11.2621 ± 0.0029	$0.0445^{+0.1313}_{-0.0445}$	SHC
2115 A	4.6375 ± 0.0252	-5.432 ± 0.019	9.584 ± 0.027	0.216	8.4507 ± 0.0028	$0.7949^{+0.3851}_{-0.3851}$	SHC
2115 B	5.0970 ± 0.1099	-4.066 ± 0.079	9.996 ± 0.204	0.698			
2127 A	6.1863 ± 0.0093	-14.002 ± 0.009	-36.751 ± 0.011	0.052	12.3582 ± 0.0028	$0.2303^{+0.0858}_{-0.1490}$	
2127 B	6.4227 ± 0.2978	-14.782 ± 0.261	-35.939 ± 0.356	1.378	18.9491 ± 0.0058		
2128 A	27.2686 ± 0.0151	-161.884 ± 0.016	-42.106 ± 0.017	0.140	7.0810 ± 0.0028	$0.0685^{+0.1156}_{-0.0605}$	
2128 B	27.2456 ± 0.0397	-165.242 ± 0.046	-44.975 ± 0.043	0.462	13.0419 ± 0.0028		
2144 A	9.4696 ± 0.0112	74.073 ± 0.014	77.519 ± 0.013	0.084	10.3998 ± 0.0028	$0.0813^{+0.1628}_{-0.0590}$	
2144 B	9.4699 ± 0.0208	75.337 ± 0.026	76.393 ± 0.023	0.061	15.1281 ± 0.0028		
2149 A	4.5418 ± 0.0145	13.482 ± 0.016	15.150 ± 0.018	0.146	10.5168 ± 0.0028	$0.6150^{+0.3468}_{-0.4568}$	
2149 B	4.5903 ± 0.0264	15.393 ± 0.027	12.735 ± 0.036	0.247	12.0274 ± 0.0028		
2152 A	3.1166 ± 0.0169	27.534 ± 0.017	-11.833 ± 0.019	0.151	11.2435 ± 0.0028	$0.7547^{+0.1955}_{-0.1955}$	SHC
2152 B	3.2220 ± 0.3165	26.996 ± 0.291	-12.013 ± 0.326	1.280	19.4442 ± 0.0040		
2169 A	2.7494 ± 0.0169	5.505 ± 0.012	-31.042 ± 0.016	0.156	10.9589 ± 0.0028		
2169 B	2.7704 ± 0.0140	5.273 ± 0.010	-30.728 ± 0.016	0.000	13.6850 ± 0.0028	$0.1838^{+0.1992}_{-0.1013}$	
2183 A	9.5169 ± 0.0190	-15.514 ± 0.020	43.704 ± 0.020	0.134	8.4875 ± 0.0028	$0.6354^{+0.3262}_{-0.3262}$	SHC
2183 B	9.5902 ± 0.0204	-21.330 ± 0.027	40.148 ± 0.021	0.156	8.8416 ± 0.0028		
2193 A	2.9294 ± 0.0094	-2.465 ± 0.009	-0.911 ± 0.011	0.050	11.8060 ± 0.0028	$0.1520^{+0.3031}_{-0.1170}$	
2193 B	2.9032 ± 0.0601	-2.530 ± 0.052	-0.987 ± 0.064	0.403	16.1816 ± 0.0029		
2195 A	5.7048 ± 0.0100	-16.224 ± 0.012	-55.807 ± 0.011	0.080	11.5123 ± 0.0028	$0.1810^{+0.2771}_{-0.1180}$	
2195 B	5.6714 ± 0.0382	-15.625 ± 0.048	-54.966 ± 0.044	0.339	15.7231 ± 0.0029		
2205 A	2.4099 ± 0.0295	-2.328 ± 0.038	27.633 ± 0.042	0.027	16.1296 ± 0.0029	$0.1342^{+0.0601}_{-0.0601}$	SHC

TABLE 1 Continued

TOI	π (mas)	$\mu_\alpha cos(\delta)$ (mas year^{-1})	μ_δ (mas year^{-1})	*epsi* (mas)	G (mag)	A_G (mag)	
2205 B	2.3861 ± 0.1390	-2.123 ± 0.165	27.466 ± 0.203	0.601	18.8104 ± 0.0035		
2205 C	2.5016 ± 0.1934	-2.725 ± 0.223	28.340 ± 0.287	0.000	19.3401 ± 0.0041		
2215 A	14.1234 ± 0.0160	-8.274 ± 0.016	-6.212 ± 0.013	0.069	10.5895 ± 0.0028		
2215 B	14.0973 ± 0.0171	-8.401 ± 0.016	-6.279 ± 0.014	0.071	10.8414 ± 0.0028	$0.0320^{+0.1923}_{-0.0107}$	
2218 B	2.8549 ± 0.0356	-17.669 ± 0.046	33.504 ± 0.040	0.388	11.9424 ± 0.0028		
2218 A	2.5423 ± 0.0110	-15.254 ± 0.014	33.429 ± 0.012	0.082	11.7408 ± 0.0028	$0.1377^{+0.2053}_{-0.1310}$	
2233 A	5.1165 ± 0.0291	1.165 ± 0.035	-24.974 ± 0.023	0.201	11.5776 ± 0.0030	$0.5892^{+0.2088}_{-0.3520}$	
2233 B	5.2052 ± 0.0379	1.061 ± 0.048	-25.646 ± 0.030	0.000	15.4905 ± 0.0029		
2239 A	2.1906 ± 0.0118	2.987 ± 0.017	-4.658 ± 0.013	0.096	11.3658 ± 0.0028		
2239 B	2.0299 ± 0.0106	2.982 ± 0.017	-4.083 ± 0.012	0.000	13.2956 ± 0.0028	$0.1557^{+0.1704}_{-0.0681}$	
2244 A	5.7439 ± 0.0188	15.007 ± 0.017	-11.535 ± 0.018	0.104	9.5576 ± 0.0029	$0.1198^{+0.1538}_{-0.1198}$	SHC
2244 B	5.7633 ± 0.0222	16.129 ± 0.019	-11.662 ± 0.018	0.119	9.9215 ± 0.0029		
2244 C	5.7981 ± 0.1555	15.022 ± 0.144	-10.886 ± 0.148	0.438	17.9098 ± 0.0033		
2246 A	4.4280 ± 0.0121	16.025 ± 0.015	51.047 ± 0.016	0.107	10.3992 ± 0.0028		
2246 B	4.4457 ± 0.0100	16.939 ± 0.013	50.845 ± 0.013	0.062	10.8843 ± 0.0028	$0.4560^{+0.2521}_{-0.2243}$	
2248 A	2.6398 ± 0.0110	3.956 ± 0.013	15.787 ± 0.014	0.000	10.7376 ± 0.0028	$0.8535^{+0.2826}_{-0.1875}$	
2248 B	2.8055 ± 0.2212	3.562 ± 0.260	15.319 ± 0.296	0.831	18.5134 ± 0.0119		
2253 A	5.8108 ± 0.0532	9.455 ± 0.056	17.639 ± 0.066	0.567	10.4163 ± 0.0028		
2253 B	6.5645 ± 0.0428	8.891 ± 0.045	17.588 ± 0.056	0.309	15.3387 ± 0.0028	$0.3200^{+0.4791}_{-0.1481}$	
2279 A	10.6363 ± 0.0097	22.635 ± 0.011	16.147 ± 0.013	0.054	10.8215 ± 0.0028	$0.1605^{+0.2243}_{-0.0848}$	
2279 B	10.6551 ± 0.0296	23.264 ± 0.036	15.201 ± 0.044	0.172	15.6025 ± 0.0029		
2281 A	5.6262 ± 0.0116	28.656 ± 0.013	-14.733 ± 0.014	0.090	9.4515 ± 0.0028		
2281 B	5.6049 ± 0.0108	28.760 ± 0.013	-13.475 ± 0.013	0.072	10.7952 ± 0.0028	$0.0600^{+0.1118}_{-0.0430}$	
2283 A	20.1663 ± 0.0123	-56.281 ± 0.016	109.172 ± 0.016	0.104	12.2841 ± 0.0028		
2283 B	20.1454 ± 0.0280	-57.264 ± 0.037	107.463 ± 0.035	0.000	15.7433 ± 0.0028	$0.1090^{+0.0897}_{-0.0321}$	
2289 A	7.1011 ± 0.0144	4.525 ± 0.016	75.018 ± 0.017	0.111	10.4503 ± 0.0028		
2289 B	7.1855 ± 0.0410	4.324 ± 0.045	75.200 ± 0.051	0.193	16.1822 ± 0.0029	$0.7560^{+0.2162}_{-0.3173}$	
2293 A	15.9360 ± 0.0156	45.215 ± 0.011	-120.703 ± 0.015	0.111	12.8578 ± 0.0028		
2293 B	16.0752 ± 0.0617	45.112 ± 0.046	-123.739 ± 0.059	0.206	16.9297 ± 0.0029	$0.3100^{+0.3101}_{-0.2540}$	
2299 A	29.1809 ± 0.0120	-14.452 ± 0.015	195.077 ± 0.015	0.085	9.2915 ± 0.0028	$0.0347^{+0.2433}_{-0.0248}$	
2299 B	29.2165 ± 0.0328	-13.038 ± 0.042	197.713 ± 0.050	0.338	12.5649 ± 0.0029		
2307 A	2.2094 ± 0.0158	21.744 ± 0.016	-20.084 ± 0.013	0.068	12.6917 ± 0.0028	$0.5075^{+0.1503}_{-0.0861}$	
2307 B	2.0919 ± 0.1416	22.161 ± 0.179	-19.523 ± 0.110	0.408	17.6546 ± 0.0054		
2321 A	8.4506 ± 0.0281	-3.922 ± 0.032	-24.932 ± 0.042	0.154	10.2853 ± 0.0028		
2321 B	8.4306 ± 0.0421	-3.760 ± 0.051	-25.597 ± 0.063	0.143	15.4528 ± 0.0028	$0.0370^{+0.1211}_{-0.0300}$	
2325 A	4.5153 ± 0.0233	-7.670 ± 0.026	-18.459 ± 0.024	0.171	9.8309 ± 0.0028	$0.1113^{+0.1734}_{-0.1113}$	SHC
2325 B	4.5677 ± 0.0401	-5.116 ± 0.041	-18.875 ± 0.036	0.208	14.7230 ± 0.0030		
2327 A	9.9809 ± 0.0105	6.518 ± 0.013	-46.525 ± 0.014	0.087	9.8614 ± 0.0028		
2327 B	9.9334 ± 0.0112	6.023 ± 0.014	-46.330 ± 0.015	0.000	13.8791 ± 0.0028	$0.2367^{+0.1853}_{-0.0824}$	

TABLE 1 Continued

TOI	π (mas)	$\mu_\alpha cos(\delta)$ (mas year^{-1})	μ_δ (mas year^{-1})	*epsi* (mas)	*G* (mag)	A_G (mag)	
2328 A	4.3202 ± 0.0090	31.870 ± 0.011	-1.815 ± 0.011	0.040	12.1029 ± 0.0028	$0.2085^{+0.1521}_{-0.1730}$	
2328 B	4.1584 ± 0.2225	31.636 ± 0.273	-0.560 ± 0.276	0.780	17.6401 ± 0.0055		
2335 A	2.1997 ± 0.0138	-4.027 ± 0.012	9.270 ± 0.016	0.112	12.5012 ± 0.0028	$0.0433^{+0.1303}_{-0.0368}$	
2335 B	2.3676 ± 0.0587	-3.618 ± 0.053	9.002 ± 0.073	0.472	16.2577 ± 0.0029		
2340 A	5.6344 ± 0.0152	59.660 ± 0.017	84.574 ± 0.020	0.079	12.3635 ± 0.0028	$0.1287^{+0.1263}_{-0.1127}$	
2340 B	5.1835 ± 0.0570	60.650 ± 0.058	83.952 ± 0.063	0.416	14.7856 ± 0.0028		
2350 A	5.3462 ± 0.0200	-5.301 ± 0.013	-8.965 ± 0.019	0.180	11.1384 ± 0.0028	$0.2785^{+0.2486}_{-0.1049}$	
2350 B	5.1138 ± 0.1399	-5.123 ± 0.087	-9.298 ± 0.129	0.619	18.2885 ± 0.0030		
2358 A	2.6084 ± 0.0180	-6.499 ± 0.019	-14.015 ± 0.019	0.094	11.8802 ± 0.0028		
2358 B	2.4728 ± 0.1570	-8.215 ± 0.162	-13.653 ± 0.137	1.138	14.3423 ± 0.0034	$0.7293^{+0.1268}_{-0.2026}$	
2374 B	7.3592 ± 0.0180	-11.470 ± 0.018	-31.421 ± 0.016	0.085	11.8186 ± 0.0028		
2374 A	7.3387 ± 0.0186	-11.949 ± 0.018	-31.746 ± 0.018	0.071	9.2231 ± 0.0028	$0.4100^{+0.2141}_{-0.2125}$	
2380 A	3.7225 ± 0.0252	2.432 ± 0.023	9.437 ± 0.019	0.105	9.8239 ± 0.0028	$0.1857^{+0.1703}_{-0.1703}$	SHC
2380 B	3.4875 ± 0.5810	1.827 ± 0.718	9.278 ± 0.437	0.000	19.5744 ± 0.0062		
2383 B	5.8490 ± 0.0182	-6.728 ± 0.017	-49.801 ± 0.013	0.093	10.9057 ± 0.0031		
2383 A	5.8524 ± 0.0169	-6.653 ± 0.016	-49.965 ± 0.012	0.082	10.3605 ± 0.0028	$0.0637^{+0.2353}_{-0.0510}$	
2384 A	5.3219 ± 0.0440	9.257 ± 0.061	-52.662 ± 0.053	0.455	14.3880 ± 0.0029	$1.4283^{+0.1100}_{-0.1100}$	SHC
2384 B	5.0517 ± 0.1666	8.013 ± 0.623	-51.041 ± 0.255	0.995	17.5517 ± 0.0051		
2409 A	5.2313 ± 0.0283	-19.893 ± 0.025	-18.523 ± 0.033	0.299	11.8352 ± 0.0028		
2409 B	5.2737 ± 0.0105	-17.476 ± 0.010	-20.485 ± 0.012	0.000	13.2702 ± 0.0028	$0.1167^{+0.1299}_{-0.0831}$	
2417 A	3.9122 ± 0.0119	33.622 ± 0.010	11.780 ± 0.013	0.094	10.7059 ± 0.0028	$0.9090^{+0.3721}_{-0.2897}$	
2417 B	3.9841 ± 0.0324	36.848 ± 0.025	11.989 ± 0.035	0.300	13.7951 ± 0.0089		
2419 A	4.0433 ± 0.0097	-12.828 ± 0.012	-19.732 ± 0.011	0.078	10.8435 ± 0.0028	$0.3953^{+0.2457}_{-0.2484}$	
2419 B	4.0702 ± 0.0334	-13.367 ± 0.048	-20.741 ± 0.037	0.293	14.6100 ± 0.0029		
2422 A	4.7712 ± 0.0251	21.109 ± 0.027	-27.759 ± 0.022	0.148	9.9060 ± 0.0028	$0.1762^{+0.0208}_{-0.0208}$	SHC5
2422 B	4.9353 ± 0.0593	21.982 ± 0.085	-29.180 ± 0.082	0.290	10.7782 ± 0.0042		
2425 A	6.2150 ± 0.0192	4.997 ± 0.022	-12.557 ± 0.020	0.094	11.7689 ± 0.0028	$0.0620^{+0.1270}_{-0.0457}$	
2425 B	6.3902 ± 0.1064	5.512 ± 0.135	-11.979 ± 0.169	0.510	16.8583 ± 0.0044		

CTOI	π (mas)	$\mu_\alpha cos(\delta)$ (mas year^{-1})	μ_δ (mas year^{-1})	*epsi* (mas)	*G* (mag)	A_G (mag)
35703676 A	2.5970 ± 0.0923	2.843 ± 0.119	-30.120 ± 0.074	0.727	12.7286 ± 0.0028	$0.0630^{+0.2071}_{-0.0407}$
35703676 B	2.8329 ± 0.0428	5.202 ± 0.052	-27.253 ± 0.031	0.000	15.8373 ± 0.0029	
83839341 A	2.7223 ± 0.0181	-33.140 ± 0.017	-26.355 ± 0.017	0.068	12.2518 ± 0.0028	$0.6090^{+0.2281}_{-0.1481}$
83839341 B	2.6648 ± 0.0207	-33.144 ± 0.020	-25.801 ± 0.019	0.089	12.2623 ± 0.0028	
98957720 A	4.7871 ± 0.0316	-42.613 ± 0.038	-3.408 ± 0.019	0.247	11.1592 ± 0.0028	
98957720 B	4.7377 ± 0.0559	-42.468 ± 0.064	-3.353 ± 0.034	0.000	16.5348 ± 0.0028	$0.3110^{+0.1541}_{-0.0211}$
105850602 AB	8.0429 ± 0.2139	-23.862 ± 0.185	-29.428 ± 0.168	1.796	8.9251 ± 0.0033	$0.0175^{+0.0726}_{-0.0122}$

TABLE 1 Continued

CTOI	π (mas)	$\mu_\alpha cos(\delta)$ (mas year^{-1})	μ_δ (mas year^{-1})	*epsi* (mas)	G (mag)	A_G (mag)	
105850602 C	6.0423 ± 0.2164	-23.125 ± 0.176	-30.583 ± 0.171	1.733	16.7498 ± 0.0033		
105850602 D	7.1762 ± 0.1470	-22.662 ± 0.091	-29.601 ± 0.112	0.571	17.0850 ± 0.0034		
117644481 A	2.9517 ± 0.0113	33.782 ± 0.009	43.201 ± 0.009	0.046	12.4883 ± 0.0028		
117644481 B	2.9461 ± 0.0555	33.909 ± 0.048	42.964 ± 0.043	0.000	16.6315 ± 0.0030	$1.9848^{+0.4293}_{-0.4761}$	
135145585 A	2.5969 ± 0.0517	-34.591 ± 0.042	2.421 ± 0.027	0.440	11.9949 ± 0.0028	$0.6600^{+0.2310}_{-0.1301}$	
135145585 B	2.7543 ± 0.0986	-30.442 ± 0.083	1.842 ± 0.060	0.000	17.6175 ± 0.0029		
139444326 A	2.0667 ± 0.0322	1.731 ± 0.022	4.759 ± 0.028	0.327	12.0059 ± 0.0028	$1.0452^{+0.3279}_{-0.4019}$	
139444326 B	2.4099 ± 0.2909	2.201 ± 0.191	4.395 ± 0.244	1.182	19.3892 ± 0.0050		
142443425 A	8.1451 ± 0.0159	-77.368 ± 0.013	34.110 ± 0.019	0.129	11.5055 ± 0.0028	$0.1930^{+0.0880}_{-0.0941}$	
142443425 B	8.1393 ± 0.0462	-75.775 ± 0.035	33.880 ± 0.047	0.383	14.6761 ± 0.0030		
144164538 A	4.7965 ± 0.0181	16.116 ± 0.019	33.129 ± 0.022	0.058	14.6250 ± 0.0028	$1.0210^{+0.4031}_{-0.1641}$	
144164538 B	4.8422 ± 0.2773	15.012 ± 0.322	33.089 ± 0.341	1.580	18.9670 ± 0.0053		
151628217 A	2.0385 ± 0.0136	3.714 ± 0.016	-5.446 ± 0.020	0.127	11.4970 ± 0.0028		
151628217 B	2.0334 ± 0.0095	4.262 ± 0.011	-6.683 ± 0.013	0.000	13.1539 ± 0.0028	$0.1683^{+0.0944}_{-0.0596}$	
152226055 A	4.2468 ± 0.0190	11.080 ± 0.016	-12.086 ± 0.014	0.103	11.7271 ± 0.0028		
152226055 B	4.2203 ± 0.0189	10.447 ± 0.016	-12.161 ± 0.014	0.000	13.8270 ± 0.0028	$0.5720^{+0.2630}_{-0.3110}$	
164781040 A	2.6525 ± 0.4136	10.367 ± 0.457	0.886 ± 0.499	4.212	14.5887 ± 0.0030		
164781040 B	1.0362 ± 0.0417	8.515 ± 0.062	3.140 ± 0.083	0.155	15.1346 ± 0.0029	$0.0000^{+0.4742}_{-0.0000}$	SHC
178367145 B	3.8421 ± 0.0302	-13.234 ± 0.030	-2.789 ± 0.022	0.203	11.7726 ± 0.0029		
178367145 A	3.9752 ± 0.0190	-13.887 ± 0.020	-2.818 ± 0.015	0.117	10.9126 ± 0.0028	$0.1957^{+0.1133}_{-0.1437}$	
197760286 A	5.4658 ± 0.1691	34.814 ± 0.178	-18.655 ± 0.131	1.392	9.9572 ± 0.0028		
197760286 B	5.1856 ± 0.0372	36.545 ± 0.043	-13.420 ± 0.029	0.081	15.5006 ± 0.0028	$0.0280^{+0.4341}_{-0.0187}$	
202712304 A	15.3450 ± 0.0168	107.379 ± 0.016	-84.082 ± 0.013	0.071	13.0651 ± 0.0028	$0.4505^{+0.4125}_{-0.3870}$	
202712304 B	14.9765 ± 0.0652	107.234 ± 0.063	-86.297 ± 0.049	0.446	15.1065 ± 0.0028		
224327878 A	8.4853 ± 0.0145	-4.061 ± 0.014	35.502 ± 0.014	0.107	11.0964 ± 0.0028	$0.0620^{+0.2797}_{-0.0540}$	
224327878 B	8.5937 ± 0.0854	-4.003 ± 0.077	37.640 ± 0.104	0.556	16.4315 ± 0.0056		
224327878 C	8.4661 ± 0.0467	-3.193 ± 0.043	35.728 ± 0.045	0.000	16.5314 ± 0.0029		
230236827 A	11.7407 ± 0.0122	5.556 ± 0.015	37.566 ± 0.017	0.119	11.6854 ± 0.0028		
230236827 B	11.7974 ± 0.0336	0.372 ± 0.045	33.544 ± 0.040	0.289	15.3282 ± 0.0028	$0.0900^{+0.2905}_{-0.0630}$	
238235254 B	2.4073 ± 0.0403	-5.316 ± 0.049	8.021 ± 0.046	0.360	6.3244 ± 0.0028		
238235254 A	2.5463 ± 0.0433	-5.435 ± 0.055	8.186 ± 0.059	0.429	6.3063 ± 0.0028	$0.0588^{+0.1099}_{-0.0393}$	
238920872 A	9.4737 ± 0.0106	10.410 ± 0.013	19.547 ± 0.013	0.053	13.1190 ± 0.0032	$0.2471^{+0.1271}_{-0.1271}$	SHC
238920872 B	9.4336 ± 0.0559	10.074 ± 0.073	19.829 ± 0.070	0.117	17.1604 ± 0.0031		
253040591 A	13.8011 ± 0.3445	25.446 ± 0.374	-35.205 ± 0.282	2.826	9.1333 ± 0.0028	$0.4387^{+0.1509}_{-0.1509}$	SHC
253040591 B	14.5199 ± 0.1306	25.997 ± 0.120	-29.287 ± 0.124	0.103	17.7513 ± 0.0031		
257605131 A	8.0993 ± 0.0108	-11.061 ± 0.010	12.347 ± 0.014	0.065	10.7561 ± 0.0028	$0.0732^{+0.1586}_{-0.0607}$	
257605131 B	8.1199 ± 0.0172	-11.481 ± 0.016	12.229 ± 0.023	0.095	14.3404 ± 0.0028		

TABLE 1 Continued

CTOI	π (mas)	$\mu_\alpha cos(\delta)$ (mas year^{-1})	μ_δ (mas year^{-1})	*epsi* (mas)	*G* (mag)	A_G (mag)	
259376845 A	3.9444 ± 0.0112	11.525 ± 0.015	-23.759 ± 0.016	0.072	12.8546 ± 0.0028		
259376845 B	3.9732 ± 0.0133	10.182 ± 0.017	-23.315 ± 0.019	0.110	12.9574 ± 0.0031	$0.5850^{+0.1238}_{-0.1631}$	
282502866 A	13.3826 ± 0.0258	-25.115 ± 0.035	-26.723 ± 0.030	0.145	7.8098 ± 0.0028		
282502866 B	13.1925 ± 0.0320	-24.914 ± 0.035	-26.448 ± 0.031	0.186	14.8252 ± 0.0028	$0.8100^{+0.0760}_{-0.1288}$	
288240183 A	6.6408 ± 0.3602	-51.336 ± 0.520	24.806 ± 0.444	3.859	9.4662 ± 0.0041	$0.3020^{+0.2134}_{-0.2134}$	SHC
288240183 B	7.0498 ± 0.0153	-46.377 ± 0.020	22.520 ± 0.020	0.123	10.6051 ± 0.0028	$0.1530^{+0.1120}_{-0.0978}$	
288240183 C	7.0320 ± 0.0574	-47.646 ± 0.108	24.037 ± 0.074	0.477	14.7007 ± 0.0032		
290596728 A	6.6127 ± 0.0186	-8.669 ± 0.015	-3.979 ± 0.013	0.087	10.7333 ± 0.0028		
290596728 B	6.6471 ± 0.0195	-8.455 ± 0.016	-3.969 ± 0.014	0.006	13.7674 ± 0.0028	$0.6563^{+0.1948}_{-0.2434}$	
300116105 A	3.2646 ± 0.0113	-1.698 ± 0.013	16.463 ± 0.013	0.079	12.1874 ± 0.0028	$0.5350^{+0.0971}_{-0.1068}$	
300116105 B	3.1741 ± 0.0817	0.148 ± 0.101	17.099 ± 0.085	0.449	17.1562 ± 0.0034		
308301091 A	4.4783 ± 0.0138	-7.295 ± 0.011	-6.361 ± 0.015	0.109	10.1343 ± 0.0028	$0.1750^{+0.1561}_{-0.1710}$	
308301091 B	4.7173 ± 0.1050	-6.105 ± 0.110	-6.001 ± 0.161	0.612	16.4662 ± 0.0079		
312091232 A	3.4329 ± 0.0169	-30.516 ± 0.021	-24.666 ± 0.015	0.084	11.7888 ± 0.0028	$0.1763^{+0.1394}_{-0.1268}$	
312091232 B	3.2928 ± 0.1112	-30.899 ± 0.130	-24.713 ± 0.098	0.129	17.4970 ± 0.0030		
326092637 A	2.5628 ± 0.0201	-9.956 ± 0.025	-16.293 ± 0.026	0.093	12.3868 ± 0.0028	$0.1720^{+0.2470}_{-0.0951}$	
326092637 B	2.5714 ± 0.4362	-9.452 ± 0.597	-15.607 ± 0.632	0.521	19.7135 ± 0.0041		
341411516 A	5.7036 ± 0.0219	30.074 ± 0.031	7.168 ± 0.029	0.260	11.1204 ± 0.0028	$0.0170^{+0.1161}_{-0.0117}$	
341411516 B	5.8132 ± 0.2458	31.061 ± 0.335	7.253 ± 0.294	0.000	19.7210 ± 0.0045		
345324572 B	19.8554 ± 0.0166	-40.646 ± 0.016	23.672 ± 0.016	0.109	13.6824 ± 0.0028		
345324572 A	19.8231 ± 0.0108	-41.421 ± 0.010	22.536 ± 0.011	0.052	9.0158 ± 0.0028	$0.2843^{+0.1402}_{-0.1894}$	
349793830 A	12.2347 ± 0.0211	-166.404 ± 0.022	-46.521 ± 0.014	0.109	9.5710 ± 0.0028	$0.0680^{+0.0783}_{-0.0261}$	
349793830 B	12.2912 ± 0.1075	-167.068 ± 0.121	-44.129 ± 0.087	0.000	17.4495 ± 0.0029		
352915304 A	8.7944 ± 0.0102	64.929 ± 0.016	151.830 ± 0.014	0.072	11.5368 ± 0.0028	$0.0980^{+0.1220}_{-0.0183}$	
352915304 B	8.7595 ± 0.0839	65.107 ± 0.138	152.160 ± 0.134	0.409	17.2980 ± 0.0041		
369376388 A	10.3996 ± 0.0104	153.458 ± 0.009	24.005 ± 0.012	0.074	11.9448 ± 0.0028	$0.6005^{+0.3379}_{-0.4346}$	
369376388 B	10.6997 ± 0.1053	150.662 ± 0.098	21.621 ± 0.117	0.766	16.8507 ± 0.0037		
369376388 C	10.3986 ± 0.0553	153.085 ± 0.053	22.296 ± 0.063	0.129	17.1337 ± 0.0029		
372913337 A	2.4642 ± 0.0158	-4.695 ± 0.020	11.038 ± 0.019	0.137	8.9919 ± 0.0028		
372913337 B	2.4294 ± 0.0114	-5.120 ± 0.014	10.868 ± 0.014	0.072	12.5578 ± 0.0028	$0.2790^{+0.2363}_{-0.1070}$	
374352402 A	2.0320 ± 0.0129	12.702 ± 0.009	-4.057 ± 0.013	0.068	12.3260 ± 0.0028	$0.3583^{+0.3858}_{-0.2818}$	
374352402 B	1.8700 ± 0.0916	12.937 ± 0.068	-4.224 ± 0.095	0.401	17.3357 ± 0.0030		
374732772 A	6.5180 ± 0.0305	-9.891 ± 0.038	-25.283 ± 0.027	0.213	10.6796 ± 0.0030	$1.2515^{+0.4256}_{-0.4849}$	
374732772 B	6.3821 ± 0.0307	-9.741 ± 0.037	-23.746 ± 0.023	0.148	14.0143 ± 0.0028		
394721720 A	2.8051 ± 0.0114	-15.344 ± 0.013	-26.763 ± 0.013	0.098	12.2568 ± 0.0028	$0.4284^{+0.1410}_{-0.1410}$	SHC
394721720 B	2.4257 ± 0.1402	-15.359 ± 0.168	-26.140 ± 0.165	0.366	18.7052 ± 0.0034		
399913539 A	3.2337 ± 0.0099	1.850 ± 0.013	28.329 ± 0.013	0.000	13.2471 ± 0.0031	$0.2455^{+0.3096}_{-0.2291}$	
399913539 B	3.3647 ± 0.0954	1.427 ± 0.141	28.147 ± 0.132	0.329	18.0096 ± 0.0031		
453455638 A	5.4637 ± 0.0172	-113.184 ± 0.023	101.703 ± 0.020	0.000	14.8091 ± 0.0028		

TABLE 1 Continued

CTOI	π (mas)	$\mu_\alpha cos(\delta)$ (mas year^{-1})	μ_δ (mas year^{-1})	*epsi* (mas)	*G* (mag)	A_G (mag)	
453455638 B	6.1329 ± 0.1091	-114.144 ± 0.149	102.925 ± 0.131	1.237	16.0432 ± 0.0037	$0.5827^{+0.1686}_{-0.2471}$	
460950389 A	6.6459 ± 0.0093	-17.586 ± 0.010	10.490 ± 0.010	0.024	12.3172 ± 0.0029	$0.5819^{+0.1431}_{-0.1431}$	SHC
460950389 B	5.3938 ± 1.3984	-17.024 ± 1.756	7.556 ± 1.400	9.219	20.7782 ± 0.0205		
467785319 A	6.4966 ± 0.0268	-1.972 ± 0.030	-30.034 ± 0.021	0.208	11.4273 ± 0.0028	$0.1590^{+0.1350}_{-0.1340}$	
467785319 B	6.2976 ± 0.1264	-0.804 ± 0.161	-28.542 ± 0.144	0.349	16.8640 ± 0.0059		
738065944 A	2.3423 ± 0.0097	35.434 ± 0.011	26.888 ± 0.011	0.053	12.7926 ± 0.0028	$0.3543^{+0.2020}_{-0.3159}$	
738065944 B	2.2919 ± 0.0120	35.904 ± 0.013	27.026 ± 0.017	0.041	13.6147 ± 0.0028		
901674675 A	2.0794 ± 0.0133	-0.017 ± 0.012	-27.116 ± 0.012	0.053	12.5042 ± 0.0028		
901674675 B	2.0663 ± 0.0162	-0.002 ± 0.014	-27.103 ± 0.014	0.088	12.7075 ± 0.0028	$0.4010^{+0.0981}_{-0.2281}$	

temperatures are available,[4] indicated by the PRI flag in Table 3. Except for the brightest and hottest companion, which is located slightly above the main sequence and exhibits a low surface gravity ($\log(g[cm/s^{-2}]) \lesssim 3.8$), i.e. this companion is a subgiant, the photometry of the majority of all detected companions is well consistent with that expected for main-sequence stars.

For two companions, namely, TOI 2001 B and TOI 2115 B no G-band photometry is listed neither in the Gaia EDR3 nor DR2, hence the properties of these companions could not be determined (indicated with the flag noGmag in Table 3).

For the remaining 34 companions, we derived their masses and effective temperatures from their absolute G-band magnitudes via interpolation (inter flag in Table 3) using the M_G-mass and M_G-T_{eff} relations from Pecaut & Mamajek (2013), adopting that these companions are main-sequence stars. In order to verify this hypothesis, we compared the obtained effective temperatures of the companions with either their Apsis-Priam temperature estimates if available, or with the effective temperatures of the companions, derived from their $(B_P - R_P)$ colors and Apsis-Priam reddening estimates $E(B_P - R_P)$ or if not available those of the associated (C)TOIs, using the $(B_P - R_P)_0$-T_{eff} relation from Pecaut & Mamajek (2013). For the temperature estimation of the companions, we have used preferably their Gaia DR2 colors if available, instead of those listed in the Gaia EDR3 because (1) the photometric passbands of both Gaia data releases are different (Lindegren et al. 2020), (2) the reddening estimates are given only in Gaia DR2 colors, and (3) the used color-temperature relation is also based on Gaia DR2 photometry.

[4]Following the recommendation of Andrae et al. (2018) Apsis-Priam temperature estimates are only used in this survey if their flags are equal to 1A000E with A and E that can have any value.

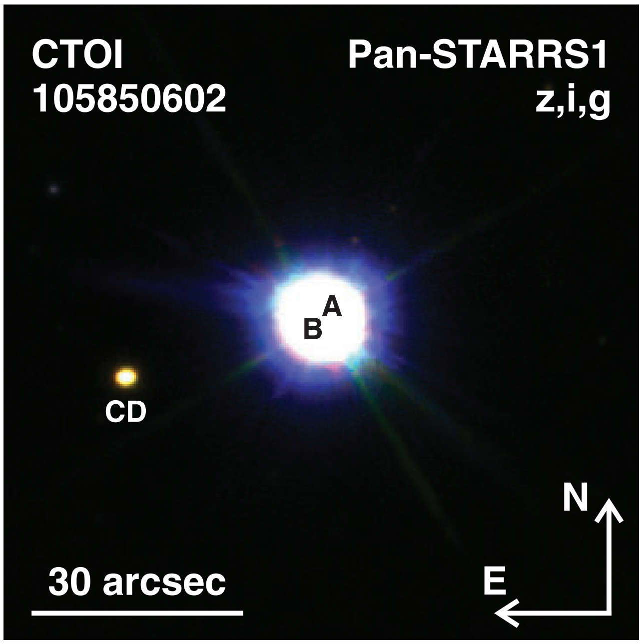

FIGURE 3 Color(RGB)-composit image of the quadruple system CTOI 105850602 AB+CD, made of z-, i-, and g-band images, taken by the Panoramic Survey Telescope and Rapid Response System (Pan-STARRS). The close binary companion (CD), whose components are separated from each other by only about 0.7 arcsec, is not resolved by Pan-STARRS but it appears clearly elongated in this image, different to other point like sources detected around the star

For all but five of these companions their effective temperatures, derived from their absolute magnitudes by assuming that they are main-sequence stars, agree well with either their Apsis-Priam temperature estimates or the temperatures, obtained from their colors. The typical deviation of the different temperature estimates is about 380 K, well consistent with the average uncertainty of the derived effective temperatures. Hence, we conclude that these companions are all main-sequence stars.

In addition, also the Gaia EDR3 ($B_P - R_P$) colors of the (C)TOIs and their companions (if available) were compared with each other, indicated by the BPRP flag in Table 3. For main-sequence stars we expect that companions, which are fainter/brighter than the (C)TOIs, appear redder/bluer than the stars and this holds for the majority

TABLE 2 This table lists for each detected companion (sorted by its identifier) the angular separation ρ and position angle *PA* to the associated (C)TOI, the difference between its parallax and that of the (C)TOI $\Delta\pi$ with its significance (in brackets calculated by taking into account also the Gaia astrometric excess noise), the differential proper motion μ_{rel} of the companion relative to the (C)TOI with its significance, as well as its *cpm-index*

TOI	ρ (arcsec)	*PA* (°)	$\Delta\pi$ (mas)	*sig*-$\Delta\pi$	μ_{rel} (mas year^{-1})	*sig*-μ_{rel}	*cpm-index*	Not in WDS
1937 B	2.48355 ± 0.00008	355.88654 ± 0.00228	0.06 ± 0.09	0.7 (0.2)	0.24 ± 0.10	2.3	104	⋆
1940 B	2.77116 ± 0.00012	242.00318 ± 0.00294	0.75 ± 0.12	6.1 (1.0)	1.78 ± 0.16	11.1	5.4	
1943 B	3.62638 ± 0.00003	114.43687 ± 0.00060	0.10 ± 0.05	2.2 (0.3)	1.04 ± 0.05	21.2	183	⋆
1946 B	2.82716 ± 0.00014	343.39102 ± 0.00338	0.60 ± 0.20	3.0 (0.4)	5.65 ± 0.22	26.1	13	
1953 B	35.95409 ± 0.00009	200.19546 ± 0.00017	0.04 ± 0.11	0.3 (0.1)	0.75 ± 0.12	6.3	21	⋆
1964 B	5.83383 ± 0.00006	53.32376 ± 0.00053	0.02 ± 0.07	0.3 (0.1)	0.19 ± 0.07	2.8	205	⋆
1966 B	33.48745 ± 0.00004	359.63816 ± 0.00007	0.42 ± 0.04	9.9 (1.5)	1.06 ± 0.04	25.2	73	⋆
1970 B	12.18765 ± 0.00005	321.04307 ± 0.00025	0.07 ± 0.09	0.7 (0.2)	0.21 ± 0.07	2.9	184	⋆
1972 B	26.20433 ± 0.00001	305.73275 ± 0.00003	0.01 ± 0.02	0.7 (0.2)	0.43 ± 0.02	22.9	163	
1984 B	3.05695 ± 0.00014	259.78789 ± 0.00245	0.03 ± 0.23	0.1 (0.0)	0.68 ± 0.17	3.9	81	⋆
1992 B	3.15370 ± 0.00002	202.28009 ± 0.00033	0.01 ± 0.03	0.3 (0.0)	0.41 ± 0.02	17.2	38	
2001 B	0.96202 ± 0.00007	280.20210 ± 0.00766	0.22 ± 0.09	2.3 (0.3)	1.50 ± 0.19	7.9	6.0	
2006 B	4.63500 ± 0.00002	246.83942 ± 0.00026	0.05 ± 0.02	2.5 (0.5)	0.68 ± 0.02	29.7	70	⋆
2009 B	9.41072 ± 0.00005	73.21041 ± 0.00023	0.02 ± 0.06	0.4 (0.1)	8.38 ± 0.05	153.5	120	
2033 B	10.65305 ± 0.00001	21.98648 ± 0.00006	0.03 ± 0.02	1.7 (0.3)	0.15 ± 0.02	9.7	343	
2036 B	4.55841 ± 0.00005	196.21520 ± 0.00055	0.11 ± 0.07	1.6 (0.3)	0.76 ± 0.06	12.1	60	⋆
2050 B	12.16939 ± 0.00004	108.63467 ± 0.00016	0.13 ± 0.04	3.5 (0.3)	4.93 ± 0.04	117.5	9.2	⋆
2056 B	4.28319 ± 0.00002	92.44090 ± 0.00027	0.01 ± 0.03	0.4 (0.1)	2.12 ± 0.02	89.0	93	
2068 B	19.98712 ± 0.00002	65.48869 ± 0.00004	0.01 ± 0.02	0.7 (0.1)	2.79 ± 0.02	140.3	143	
2072 B	2.98886 ± 0.00002	130.50157 ± 0.00043	0.07 ± 0.03	2.7 (0.3)	4.80 ± 0.03	147.7	86	
2084 B	12.24533 ± 0.00057	191.19264 ± 0.00314	0.04 ± 0.75	0.1 (0.0)	2.54 ± 0.93	2.7	48	⋆
2092 B	2.70349 ± 0.00062	272.26872 ± 0.01306	1.46 ± 0.71	2.1 (1.0)	1.60 ± 0.77	2.1	126	⋆
2094 B	10.71371 ± 0.00011	215.71577 ± 0.00062	0.15 ± 0.12	1.3 (0.2)	1.67 ± 0.15	11.0	66	⋆
2106 B	2.87903 ± 0.00035	1.74172 ± 0.00667	0.17 ± 0.46	0.4 (0.0)	4.15 ± 0.40	10.5	33	⋆
2108 B	1.19997 ± 0.00003	185.80397 ± 0.00356	0.00 ± 0.06	0.1 (0.0)	0.82 ± 0.06	12.8	19	⋆
2113 B	1.41338 ± 0.00003	274.78287 ± 0.00130	0.02 ± 0.03	0.8 (0.1)	1.46 ± 0.04	33.4	86	
2115 B	0.95546 ± 0.00007	88.20173 ± 0.00946	0.46 ± 0.11	4.1 (0.6)	1.43 ± 0.10	14.6	15	
2127 B	2.66269 ± 0.00028	185.95004 ± 0.00475	0.24 ± 0.30	0.8 (0.2)	1.13 ± 0.31	3.6	69	
2128 B	6.49976 ± 0.00004	196.73203 ± 0.00030	0.02 ± 0.04	0.5 (0.0)	4.42 ± 0.05	92.6	77	
2144 B	14.70306 ± 0.00002	227.52790 ± 0.00008	0.00 ± 0.02	0.0 (0.0)	1.69 ± 0.03	60.0	127	
2149 B	1.61679 ± 0.00003	110.20239 ± 0.00108	0.05 ± 0.03	1.6 (0.2)	3.08 ± 0.04	83.0	13	
2152 B	20.59743 ± 0.00025	302.41777 ± 0.00070	0.11 ± 0.32	0.3 (0.1)	0.57 ± 0.30	1.9	105	⋆
2169 B	6.45111 ± 0.00001	233.68918 ± 0.00015	0.02 ± 0.02	1.0 (0.1)	0.39 ± 0.02	19.1	161	⋆
2183 B	1.58405 ± 0.00002	164.18066 ± 0.00086	0.07 ± 0.03	2.6 (0.4)	6.82 ± 0.03	210.3	13	

TABLE 2 Continued

TOI	ρ (arcsec)	*PA* (°)	$\Delta\pi$ (mas)	*sig*-$\Delta\pi$	μ_{rel} (mas year^{-1})	*sig*-μ_{rel}	*cpm*-*index*	Not in WDS
2193 B	1.86909 ± 0.00005	124.24580 ± 0.00160	0.03 ± 0.06	0.4 (0.1)	0.10 ± 0.06	1.7	53	⋆
2195 B	3.34320 ± 0.00004	210.34890 ± 0.00064	0.03 ± 0.04	0.8 (0.1)	1.03 ± 0.05	22.1	112	⋆
2205 B	21.83293 ± 0.00014	255.40300 ± 0.00039	0.02 ± 0.14	0.2 (0.0)	0.26 ± 0.19	1.4	209	⋆
2205 C	2.14975 ± 0.00018	83.39429 ± 0.00570	0.09 ± 0.20	0.5 (0.5)	0.81 ± 0.28	2.9	69	⋆
2215 B	62.61249 ± 0.00002	223.79323 ± 0.00002	0.03 ± 0.02	1.1 (0.3)	0.14 ± 0.02	6.6	145	⋆
2218 A	6.82084 ± 0.00004	269.12176 ± 0.00030	0.31 ± 0.04	8.4 (0.8)	2.42 ± 0.05	50.3	31	
2233 B	4.47377 ± 0.00003	188.08418 ± 0.00054	0.09 ± 0.05	1.9 (0.4)	0.68 ± 0.04	17.7	75	⋆
2239 B	18.77303 ± 0.00002	233.49052 ± 0.00005	0.16 ± 0.02	10.1 (1.7)	0.58 ± 0.02	32.5	18	⋆
2244 B	1.50266 ± 0.00002	49.25479 ± 0.00077	0.02 ± 0.03	0.7 (0.1)	1.13 ± 0.03	44.3	34	
2244 C	20.32665 ± 0.00012	307.25633 ± 0.00033	0.05 ± 0.16	0.3 (0.1)	0.65 ± 0.15	4.4	58	⋆
2246 B	5.84629 ± 0.00002	339.01233 ± 0.00015	0.02 ± 0.02	1.1 (0.1)	0.94 ± 0.02	47.1	114	
2248 B	3.29667 ± 0.00021	49.71924 ± 0.00369	0.17 ± 0.22	0.7 (0.2)	0.61 ± 0.28	2.2	52	⋆
2253 B	26.26311 ± 0.00006	291.05107 ± 0.00015	0.75 ± 0.07	11.0 (1.2)	0.57 ± 0.07	7.9	70	⋆
2279 B	4.57139 ± 0.00003	319.06660 ± 0.00037	0.02 ± 0.03	0.6 (0.1)	1.14 ± 0.04	26.1	49	⋆
2281 B	33.97687 ± 0.00002	206.74198 ± 0.00002	0.02 ± 0.02	1.3 (0.2)	1.26 ± 0.02	66.1	51	
2283 B	26.52255 ± 0.00003	336.13432 ± 0.00007	0.02 ± 0.03	0.7 (0.2)	1.97 ± 0.04	50.6	124	
2289 B	12.66428 ± 0.00004	131.12439 ± 0.00018	0.08 ± 0.04	1.9 (0.4)	0.27 ± 0.05	5.4	555	⋆
2293 B	4.66336 ± 0.00005	1.24380 ± 0.00045	0.14 ± 0.06	2.2 (0.6)	3.04 ± 0.06	49.9	86	⋆
2299 B	3.60503 ± 0.00003	280.93394 ± 0.00056	0.04 ± 0.03	1.0 (0.1)	2.99 ± 0.05	59.1	132	
2307 B	2.91691 ± 0.00009	205.82182 ± 0.00202	0.12 ± 0.14	0.8 (0.3)	0.70 ± 0.14	5.0	85	⋆
2321 B	21.37467 ± 0.00003	150.86054 ± 0.00009	0.02 ± 0.05	0.4 (0.1)	0.68 ± 0.07	9.1	75	⋆
2325 B	4.52007 ± 0.00003	300.86111 ± 0.00045	0.05 ± 0.05	1.1 (0.2)	2.59 ± 0.05	53.4	15	⋆
2327 B	38.79962 ± 0.00002	156.28735 ± 0.00002	0.05 ± 0.02	3.1 (0.5)	0.53 ± 0.02	27.6	176	
2328 B	1.63846 ± 0.00023	258.49775 ± 0.00812	0.16 ± 0.22	0.7 (0.2)	1.28 ± 0.28	4.6	50	⋆
2335 B	3.87308 ± 0.00005	304.83135 ± 0.00073	0.17 ± 0.06	2.8 (0.3)	0.49 ± 0.06	8.0	41	⋆
2340 B	9.97872 ± 0.00005	125.88685 ± 0.00029	0.45 ± 0.06	7.6 (1.1)	1.17 ± 0.06	18.8	177	⋆
2250 B	31.40562 ± 0.00005	269.01582 ± 0.00019	0.23 ± 0.14	1.6 (0.4)	0.38 ± 0.12	3.1	56	⋆
2358 B	7.30773 ± 0.00012	139.11250 ± 0.00091	0.14 ± 0.16	0.9 (0.1)	1.75 ± 0.16	10.8	18	⋆
2374 A	22.34477 ± 0.00002	46.57715 ± 0.00005	0.02 ± 0.03	0.8 (0.2)	0.58 ± 0.03	23.1	116	
2380 B	5.07723 ± 0.00047	256.80573 ± 0.00470	0.24 ± 0.58	0.4 (0.4)	0.63 ± 0.70	0.9	31	⋆
2383 A	24.09397 ± 0.00002	39.17459 ± 0.00005	0.00 ± 0.02	0.1 (0.0)	0.18 ± 0.02	9.6	558	
2384 B	0.83848 ± 0.00020	350.29022 ± 0.02994	0.27 ± 0.17	1.6 (0.2)	2.04 ± 0.43	4.7	51	⋆
2409 B	23.83756 ± 0.00002	270.74528 ± 0.00006	0.04 ± 0.03	1.4 (0.1)	3.11 ± 0.03	102.3	17	⋆
2417 B	1.85419 ± 0.00002	285.16794 ± 0.00090	0.07 ± 0.03	2.1 (0.2)	3.23 ± 0.03	119.8	23	⋆
2419 B	1.71429 ± 0.00003	331.75352 ± 0.00133	0.03 ± 0.03	0.8 (0.1)	1.14 ± 0.04	27.7	42	⋆

TABLE 2 Continued

TOI	ρ (arcsec)	*PA* (°)	$\Delta\pi$ (mas)	*sig*-$\Delta\pi$	μ_{rel} (mas year^{-1})	*sig*-μ_{rel}	*cpm-index*	Not in WDS
2422 B	0.85018 ± 0.00007	140.97694 ± 0.00437	0.16 ± 0.06	2.5 (0.5)	1.67 ± 0.09	19.4	43	
2425 B	2.30113 ± 0.00009	72.60363 ± 0.00229	0.18 ± 0.11	1.6 (0.3)	0.77 ± 0.16	5.0	34	⋆
CTOI	**ρ (arcsec)**	***PA* (°)**	**$\Delta\pi$ (mas)**	***sig*-$\Delta\pi$**	**μ_{rel} (mas year^{-1})**	***sig*-μ_{rel}**	***cpm-index***	**Not in WDS**
35703676 B	8.45241 ± 0.00008	71.11569 ± 0.00045	0.24 ± 0.10	2.3 (0.3)	3.71 ± 0.10	36.0	16	⋆
83839341 B	5.56932 ± 0.00002	207.66328 ± 0.00026	0.06 ± 0.03	2.1 (0.5)	0.55 ± 0.03	21.7	152	⋆
98957720 B	16.06523 ± 0.00004	231.40252 ± 0.00014	0.05 ± 0.06	0.8 (0.2)	0.16 ± 0.07	2.2	550	⋆
105850602 C	29.25593 ± 0.00023	106.60682 ± 0.00041	2.00 ± 0.30	6.6 (0.8)	1.37 ± 0.24	5.6	56	⋆
105850602 D	28.57790 ± 0.00018	106.83131 ± 0.00036	0.87 ± 0.26	3.3 (0.5)	1.21 ± 0.21	5.9	62	⋆
117644481 B	15.28674 ± 0.00004	224.70015 ± 0.00014	0.01 ± 0.06	0.1 (0.1)	0.27 ± 0.05	6.0	408	⋆
135145585 B	11.11883 ± 0.00006	29.94000 ± 0.00040	0.16 ± 0.11	1.4 (0.3)	4.19 ± 0.09	45.3	16	⋆
139444326 B	6.38457 ± 0.00020	174.59532 ± 0.00130	0.34 ± 0.29	1.2 (0.3)	0.59 ± 0.21	2.8	17	⋆
142443425 B	3.16439 ± 0.00003	115.19061 ± 0.00072	0.01 ± 0.05	0.1 (0.0)	1.61 ± 0.04	42.7	104	⋆
144164538 B	1.69843 ± 0.00028	48.92419 ± 0.00936	0.05 ± 0.28	0.2 (0.0)	1.10 ± 0.32	3.4	66	⋆
151628217 B	14.42224 ± 0.00002	213.85689 ± 0.00006	0.01 ± 0.02	0.3 (0.0)	1.35 ± 0.02	58.4	11	⋆
152226055 B	16.03023 ± 0.00002	319.68424 ± 0.00006	0.03 ± 0.03	1.0 (0.2)	0.64 ± 0.02	28.2	51	⋆
164781040 B	0.88788 ± 0.00038	47.48872 ± 0.02454	1.62 ± 0.42	3.9 (0.4)	2.92 ± 0.49	6.0	6.6	
178367145 A	4.86196 ± 0.00002	318.91640 ± 0.00029	0.13 ± 0.04	3.7 (0.6)	0.65 ± 0.04	18.1	42	
197760286 B	5.80368 ± 0.00013	243.46265 ± 0.00105	0.28 ± 0.17	1.6 (0.2)	5.51 ± 0.14	39.5	14	⋆
202712304 B	15.70443 ± 0.00004	221.78081 ± 0.00014	0.37 ± 0.07	5.5 (0.8)	2.22 ± 0.05	43.7	123	
224327878 B	2.26527 ± 0.00006	98.18354 ± 0.00250	0.11 ± 0.09	1.3 (0.2)	2.14 ± 0.10	20.4	34	⋆
224327878 C	10.28639 ± 0.00004	35.10678 ± 0.00021	0.02 ± 0.05	0.4 (0.2)	0.90 ± 0.05	19.8	80	⋆
230236827 B	4.15576 ± 0.00003	343.54497 ± 0.00047	0.06 ± 0.04	1.6 (0.2)	6.56 ± 0.05	142.7	11	⋆
238235254 A	16.42331 ± 0.00006	227.56205 ± 0.00020	0.14 ± 0.06	2.3 (0.2)	0.20 ± 0.07	2.7	96	
238920872 B	45.59533 ± 0.00006	121.75295 ± 0.00007	0.04 ± 0.06	0.7 (0.3)	0.44 ± 0.07	6.0	101	⋆
253040591 B	8.83229 ± 0.00027	221.32306 ± 0.00178	0.72 ± 0.37	2.0 (0.3)	5.94 ± 0.31	19.2	14	⋆
257605131 B	37.81874 ± 0.00002	239.83724 ± 0.00003	0.02 ± 0.02	1.0 (0.2)	0.44 ± 0.02	22.3	76	⋆
259376845 B	4.64337 ± 0.00002	242.40365 ± 0.00021	0.03 ± 0.02	1.7 (0.2)	1.41 ± 0.02	61.8	37	⋆
282502866 B	45.17057 ± 0.00004	41.42217 ± 0.00005	0.19 ± 0.04	4.6 (0.8)	0.34 ± 0.05	7.5	214	⋆
288240183 B	60.05636 ± 0.00036	332.60249 ± 0.00036	0.41 ± 0.36	1.1 (0.1)	5.46 ± 0.51	10.8	20	
288240183 C	58.24718 ± 0.00036	332.54920 ± 0.00037	0.39 ± 0.36	1.1 (0.1)	3.77 ± 0.53	7.1	29	⋆
290596728 B	5.41246 ± 0.00002	135.75015 ± 0.00020	0.03 ± 0.03	1.3 (0.4)	0.21 ± 0.02	9.8	88	⋆
300116105 B	2.41041 ± 0.00008	277.14941 ± 0.00162	0.09 ± 0.08	1.1 (0.2)	1.95 ± 0.10	19.5	17	⋆
308301091 B	3.20160 ± 0.00009	31.36135 ± 0.00133	0.24 ± 0.11	2.3 (0.4)	1.24 ± 0.12	10.7	15	⋆
312091232 B	7.79773 ± 0.00010	56.36780 ± 0.00069	0.14 ± 0.11	1.2 (0.7)	0.39 ± 0.13	2.9	204	⋆
326092637 B	20.85385 ± 0.00027	16.93096 ± 0.00093	0.01 ± 0.44	0.0 (0.0)	0.85 ± 0.62	1.4	44	⋆

TABLE 2 Continued

CTOI	ρ (arcsec)	*PA* (°)	$\Delta\pi$ (mas)	*sig*-$\Delta\pi$	μ_{rel} (mas year^{-1})	*sig*-μ_{rel}	*cpm-index*	Not in WDS
341411516 B	23.73899 ± 0.00024	105.66263 ± 0.00061	0.11 ± 0.25	0.4 (0.3)	0.99 ± 0.34	2.9	63	★
345324572 A	32.07658 ± 0.00002	19.00568 ± 0.00003	0.03 ± 0.02	1.6 (0.3)	1.38 ± 0.02	71.5	68	★
349793830 B	28.23873 ± 0.00009	264.01259 ± 0.00016	0.06 ± 0.11	0.5 (0.4)	2.48 ± 0.09	27.3	139	
352915304 B	3.75547 ± 0.00009	206.52765 ± 0.00136	0.03 ± 0.08	0.4 (0.1)	0.37 ± 0.14	2.8	882	
369376388 B	1.63306 ± 0.00008	242.28326 ± 0.00304	0.30 ± 0.11	2.8 (0.4)	3.67 ± 0.11	34.4	84	★
369376388 C	23.83109 ± 0.00005	39.23375 ± 0.00011	0.00 ± 0.06	0.0 (0.0)	1.75 ± 0.06	27.5	177	
372913337 B	14.59903 ± 0.00002	322.97056 ± 0.00007	0.03 ± 0.02	1.8 (0.2)	0.46 ± 0.02	18.8	52	★
374352402 B	4.11475 ± 0.00005	252.26653 ± 0.00097	0.16 ± 0.09	1.8 (0.4)	0.29 ± 0.08	3.7	93	★
374732772 B	5.05320 ± 0.00003	328.64658 ± 0.00041	0.14 ± 0.04	3.1 (0.5)	1.54 ± 0.04	43.3	34	★
394721720 B	11.33222 ± 0.00013	151.28537 ± 0.00068	0.38 ± 0.14	2.7 (0.9)	0.62 ± 0.17	3.8	98	★
399913539 B	5.24516 ± 0.00009	136.57882 ± 0.00100	0.13 ± 0.10	1.4 (0.4)	0.46 ± 0.14	3.3	123	★
453455638 B	10.42144 ± 0.00011	83.96279 ± 0.00057	0.67 ± 0.11	6.1 (0.5)	1.55 ± 0.14	11.1	197	★
460950389 B	54.01510 ± 0.00121	202.76271 ± 0.00130	1.25 ± 1.40	0.9 (0.1)	2.99 ± 1.41	2.1	13	★
467785319 B	3.20547 ± 0.00012	24.51624 ± 0.00263	0.20 ± 0.13	1.5 (0.5)	1.89 ± 0.15	12.4	31	★
738065944 B	2.00627 ± 0.00001	276.64459 ± 0.00043	0.05 ± 0.02	3.3 (0.7)	0.49 ± 0.02	28.3	183	★
901674675 B	2.34422 ± 0.00002	217.51342 ± 0.00037	0.01 ± 0.02	0.6 (0.1)	0.02 ± 0.02	1.1	2732	★

Note: The last column indicates (★) if the detected companion is not listed in the WDS as companion(−candidate) of the (C)TOI.

TABLE 3 This table lists the equatorial coordinates (α, δ for epoch 2016.0) of all detected co-moving companions (sorted by their identifiers) together with their derived absolute G-band magnitudes M_G, masses, and effective temperatures T_{eff}

TOI	α (°)	δ (°)	M_G (mag)	*sep* (au)	*mass* ($M_\odot$)	T_{eff} (K)	Flags
1937 B	116.37063898358	−52.38256904657	$7.62^{+0.17}_{-0.24}$	1,030	$0.59^{+0.02}_{-0.05}$	$4,177^{+276}_{-250}$	`BPRP`
1940 B	212.64705044663	−27.99343384615	$5.60^{+0.21}_{-0.21}$	739	$0.85^{+0.04}_{-0.06}$	$5,200^{+124}_{-120}$	`inter EDR3`
1943 B	183.70611541557	−63.08713763185	$7.81^{+0.11}_{-0.09}$	473	$0.50^{+0.01}_{-0.01}$	$4,411^{+168}_{-157}$	`BPRP`
1946 B	217.27930985483	−43.36122919815	$5.09^{+0.18}_{-0.22}$	709	$0.87^{+0.09}_{-0.07}$	$5,714^{+386}_{-380}$	
1953 B	215.14092879184	−41.99269221369	$10.26^{+0.18}_{-0.09}$	9,463	$0.35^{+0.05}_{-0.01}$	$3,318^{+59}_{-48}$	`BPRP`
1964 B	201.64389030315	−39.62891769667	$7.83^{+0.03}_{-0.12}$	2,326	$0.55^{+0.01}_{-0.02}$	$4,193^{+307}_{-214}$	`BPRP`
1966 B	209.98243641458	−43.31801392589	$6.11^{+0.29}_{-0.18}$	8,975	$0.79^{+0.04}_{-0.03}$	$4,906^{+192}_{-84}$	`BPRP PRI`
1970 B	190.71676597317	−53.68567116786	$9.08^{+0.23}_{-0.30}$	5,025	$0.50^{+0.01}_{-0.05}$	$3,550^{+64}_{-57}$	`BPRP`
1972 B	176.05846644906	−59.90759743827	$3.89^{+0.07}_{-0.26}$	5,179	$1.07^{+0.12}_{-0.12}$	$6,277^{+362}_{-315}$	`BPRP PRI`
1984 B	168.87036013723	−44.42914110070	$11.12^{+0.03}_{-0.13}$	756	$0.24^{+0.01}_{-0.01}$	$3,228^{+13}_{-3}$	`inter EDR3 BPRP`
1992 B	162.91641069316	−44.98555236333	$3.42^{+0.37}_{-0.26}$	1,213	$1.14^{+0.19}_{-0.17}$	$6,381^{+560}_{-490}$	`BPRP PRI`
2001 B	128.18085020302	−58.57546310498		433			`EDR3 noGmag`
2006 B	91.22129476743	−69.36082554536	$4.21^{+0.19}_{-0.13}$	2,305	$1.00^{+0.10}_{-0.10}$	$6,135^{+371}_{-325}$	`BPRP PRI`
2009 B	16.91102529334	22.95355541328	$10.88^{+0.18}_{-0.17}$	193	$0.33^{+0.01}_{-0.01}$	$3,072^{+29}_{-31}$	`BPRP PRI`

TABLE 3 Continued

TOI	α (°)	δ (°)	M_G (mag)	*sep* (au)	*mass* ($M_\odot$)	T_{eff} (K)	Flags
2033 B	17.68275285338	65.25239187480	$3.36^{+0.34}_{-0.37}$	3,009	$1.18^{+0.17}_{-0.16}$	$6,372^{+547}_{-423}$	BPRP PRI
2036 B	233.01453280974	24.08380188116	$7.33^{+0.48}_{-0.30}$	1,032	$0.55^{+0.01}_{-0.01}$	$5,038^{+69}_{-188}$	BPRP
2050 B	323.91600940223	65.43645611145	$8.24^{+0.14}_{-0.29}$	1,391	$0.55^{+0.01}_{-0.01}$	$3,881^{+52}_{-32}$	BPRP PRI
2056 B	2.60181476661	58.48938732348	$7.14^{+0.14}_{-0.17}$	397	$0.61^{+0.04}_{-0.01}$	$4,600^{+357}_{-199}$	BPRP
2068 B	186.28373776065	60.42064810535	$8.80^{+0.17}_{-0.36}$	1,059	$0.55^{+0.01}_{-0.01}$	$3,572^{+45}_{-31}$	BPRP PRI
2072 B	173.98897259356	75.54607768850	$10.44^{+0.11}_{-0.12}$	117	$0.35^{+0.04}_{-0.01}$	$3,247^{+246}_{-51}$	BPRP PRI
2084 B	259.25233532656	72.74369142724	$15.37^{+0.02}_{-0.12}$	1,399	$0.09^{+0.01}_{-0.01}$	$2,590^{+18}_{-5}$	inter BPRP
2092 B	212.54643389257	45.56389415042	$13.05^{+0.08}_{-0.10}$	479			WD EDR3 BPRP
2094 B	254.13742491435	70.02489938048	$14.19^{+0.05}_{-0.14}$	538	$0.11^{+0.01}_{-0.01}$	$2,894^{+21}_{-8}$	inter BPRP
2106 B	207.17848145517	44.91254228578	$8.77^{+0.10}_{-0.10}$	346	$0.50^{+0.01}_{-0.01}$	$3,724^{+24}_{24}$	inter BPRP
2108 B	247.48156446857	21.49483143158	$3.11^{+0.27}_{-0.41}$	303	$0.95^{+0.30}_{-0.19}$	$5,954^{+800}_{740}$	
2113 B	267.35407815488	40.45712910786	$4.21^{+0.05}_{-0.14}$	360	$1.00^{+0.10}_{-0.11}$	$6,384^{+350}_{299}$	BPRP
2115 B	19.59598675578	63.54509607880		206			EDR3 noGmag
2127 B	256.34628231343	33.01158434380	$12.68^{+0.15}_{-0.09}$	430			WD EDR3 BPRP
2128 B	256.98115969078	32.10356773055	$9.41^{+0.07}_{-0.12}$	238	$0.36^{+0.04}_{-0.01}$	$3,748^{+229}_{-161}$	BPRP
2144 B	350.23675703392	79.43903525527	$9.90^{+0.06}_{-0.17}$	1,553	$0.40^{+0.01}_{-0.01}$	$3,360^{+35}_{-37}$	BPRP PRI
2149 B	285.59708263433	42.50726078542	$5.51^{+0.46}_{-0.35}$	356	$0.81^{+0.21}_{-0.19}$	$5,425^{+776}_{-1052}$	
2152 B	26.31614962469	77.79318868748	$11.16^{+0.20}_{-0.20}$	6,609	$0.24^{+0.02}_{-0.02}$	$3,223^{+20}_{-20}$	inter BPRP
2169 B	279.16854084831	23.25755382074	$5.52^{+0.11}_{-0.20}$	2,346	$0.83^{+0.05}_{-0.05}$	$5,374^{+262}_{-206}$	BPRP PRI
2183 B	283.48984559533	37.38040766442	$2.77^{+0.33}_{-0.33}$	166	$1.39^{+0.25}_{-0.25}$	$7,066^{+1196}_{-812}$	BPRP
2193 B	313.69268269724	−72.80493275516	$9.65^{+0.12}_{-0.31}$	638	$0.40^{+0.16}_{-0.14}$	$3,541^{+496}_{-312}$	
2195 B	34.83851060185	−72.70970300127	$7.83^{+0.12}_{-0.28}$	586	$0.55^{+0.04}_{-0.04}$	$4,119^{+150}_{-250}$	BPRP
2205 B	94.30504481936	−56.51138346415	$10.59^{+0.07}_{-0.07}$	9,060	$0.30^{+0.01}_{-0.01}$	$3,308^{+13}_{-13}$	inter BPRP
2205 C	94.31675618323	−56.50978635189	$11.12^{+0.07}_{-0.07}$	892	$0.24^{+0.01}_{-0.01}$	$3,228^{+7}_{-7}$	inter BPRP
2215 B	286.05887028356	−32.36683422030	$6.49^{+0.02}_{-0.20}$	4,433	$0.73^{+0.02}_{-0.03}$	$4,759^{+182}_{-187}$	BPRP PRI
2218 A	107.15134082021	−64.23282491835	$3.64^{+0.14}_{-0.21}$	2,389	$1.08^{+0.16}_{-0.13}$	$6,299^{+477}_{-395}$	BPRP PRI
2233 B	296.91945139989	−32.57720015101	$8.22^{+0.36}_{-0.21}$	874	$0.54^{+0.01}_{-0.02}$	$3,950^{+41}_{-29}$	BPRP
2239 B	65.39925931554	−67.47014069910	$4.49^{+0.07}_{-0.18}$	8,570	$0.93^{+0.08}_{-0.09}$	$6,125^{+266}_{-230}$	BPRP PRI
2244 B	308.56398032092	−48.27456998081	$3.00^{+0.13}_{-0.16}$	262	$1.35^{+0.20}_{-0.24}$	$7,145^{+1156}_{-777}$	BPRP
2244 C	308.55675305431	−48.27142425630	$11.52^{+0.12}_{-0.16}$	3,539	$0.25^{+0.01}_{-0.05}$	$3,041^{+13}_{-40}$	BPRP
2246 B	113.04208107725	−65.80987155300	$3.76^{+0.23}_{-0.26}$	1,320	$1.08^{+0.13}_{-0.13}$	$6,346^{+386}_{-334}$	BPRP PRI
2248 B	80.62608655037	−70.25373433972	$9.77^{+0.19}_{-0.29}$	1,249	$0.39^{+0.04}_{-0.02}$	$3,478^{+55}_{-46}$	inter EDR3 BPRP
2253 B	276.84450187297	73.26719741598	$9.28^{+0.15}_{-0.48}$	4,520	$0.50^{+0.01}_{-0.01}$	$3,428^{+47}_{-9}$	BPRP PRI
2279 B	255.24461493115	45.38724425492	$9.35^{+0.09}_{-0.23}$	430	$0.40^{+0.01}_{-0.02}$	$3,687^{+151}_{-194}$	BPRP
2281 B	294.37931940875	66.96300161303	$4.48^{+0.05}_{-0.12}$	6,039	$0.98^{+0.07}_{-0.10}$	$6,027^{+275}_{-280}$	BPRP PRI
2283 B	248.32656847020	63.53124834111	$12.24^{+0.04}_{-0.09}$	1,315	$0.19^{+0.01}_{-0.07}$	$2,909^{+13}_{-14}$	BPRP PRI
2289 B	255.10100397713	39.72794649361	$10.35^{+0.32}_{-0.22}$	1,783	$0.40^{+0.01}_{-0.01}$	$3,139^{+31}_{-11}$	BPRP PRI
2293 B	115.59347921340	70.40535489770	$12.43^{+0.26}_{-0.32}$	293	$0.16^{+0.01}_{-0.01}$	$2,983^{+8}_{-56}$	BPRP PRI
2299 B	286.22240974084	79.75619277781	$8.88^{+0.03}_{-0.25}$	124	$0.45^{+0.04}_{-0.01}$	$3,830^{+193}_{-110}$	BPRP

TABLE 3 Continued

TOI	α (°)	δ (°)	M_G (mag)	*sep* (au)	*mass* ($M_\odot$)	T_{eff} (K)	Flags
2307 B	330.13554334398	−29.14932158011	$8.87^{+0.09}_{-0.16}$	1,320	$0.49^{+0.02}_{-0.01}$	$3,700^{+39}_{-18}$	`inter BPRP`
2321 B	196.73942411562	16.54415038318	$10.13^{+0.04}_{-0.13}$	2,529	$0.38^{+0.01}_{-0.08}$	$3,305^{+12}_{-37}$	`BPRP PRI`
2325 B	343.54329331845	−36.28713515058	$6.94^{+0.12}_{-0.18}$	1,001	$0.60^{+0.04}_{-0.01}$	$4,829^{+206}_{-256}$	`BPRP`
2327 B	103.43704505805	−73.08558755467	$8.79^{+0.09}_{-0.19}$	3,887	$0.55^{+0.01}_{-0.01}$	$3,592^{+68}_{-37}$	`BPRP PRI`
2328 B	31.68784113786	−81.24746699057	$10.61^{+0.18}_{-0.16}$	379	$0.29^{+0.02}_{-0.02}$	$3,305^{+30}_{-34}$	`inter EDR3 BPRP`
2335 B	50.82546214680	−40.45290191998	$7.93^{+0.04}_{-0.14}$	1,761	$0.57^{+0.02}_{-0.01}$	$3,966^{+47}_{-15}$	`inter BPRP`
2340 B	42.26379287408	−16.55926854837	$8.40^{+0.12}_{-0.13}$	1,771	$0.60^{+0.03}_{-0.01}$	$3,661^{+90}_{-153}$	`BPRP PRI`
2350 B	97.39871390344	−21.99453651654	$11.65^{+0.11}_{-0.25}$	5,874	$0.20^{+0.02}_{-0.01}$	$3,159^{+40}_{-17}$	`inter BPRP`
2358 B	196.28739985402	−31.98691483902	$5.32^{+0.21}_{-0.13}$	2,802	$0.73^{+0.08}_{-0.04}$	$5,716^{+255}_{-727}$	`BPRP PRI`
2374 A	319.50310270344	−22.04556079240	$3.50^{+0.22}_{-0.22}$	3,036	$1.17^{+0.17}_{-0.16}$	$6,343^{+585}_{-478}$	`BPRP PRI`
2380 B	0.32437138931	−8.92657181230	$12.24^{+0.18}_{-0.18}$	1,364	$0.17^{+0.01}_{-0.01}$	$3,071^{+23}_{-23}$	`inter EDR3`
2383 A	1.48935329659	−20.64877382679	$4.10^{+0.06}_{-0.24}$	4,119	$1.04^{+0.11}_{-0.11}$	$6,118^{+345}_{-275}$	`BPRP PRI`
2384 B	36.15605640406	−64.99997342715	$11.39^{+0.12}_{-0.12}$	158	$0.20^{+0.13}_{-0.07}$	$3,170^{+292}_{-293}$	
2409 B	44.32959674872	−41.19168974979	$6.75^{+0.09}_{-0.14}$	4,557	$0.70^{+0.01}_{-0.02}$	$4,609^{+210}_{-175}$	`BPRP PRI`
2417 B	37.88458406443	−40.01606774547	$5.85^{+0.29}_{-0.38}$	474	$0.79^{+0.09}_{-0.03}$	$5,060^{+239}_{-143}$	`inter`
2419 B	53.26996227934	−56.58801950869	$8.52^{+0.25}_{-0.25}$	424	$0.52^{+0.16}_{-0.18}$	$3,853^{+867}_{-428}$	
2422 B	24.88466502593	−7.39491592998	$4.00^{+0.03}_{-0.03}$	178	$1.15^{+0.01}_{-0.01}$	$6,091^{+24}_{-24}$	`inter EDR3 BPRP`
2425 B	19.13130751686	−0.28991369508	$9.60^{+0.05}_{-0.13}$	370	$0.35^{+0.05}_{-0.05}$	$3,612^{+204}_{-177}$	`BPRP`

CTOI	α (°)	δ (°)	M_G (mag)	*sep* (au)	*mass* ($M_\odot$)	T_{eff} (K)	Flags
35703676 B	23.79838607967	−0.88660913129	$7.60^{+0.09}_{-0.23}$	3,255	$0.65^{+0.04}_{-0.03}$	$3,823^{+50}_{-197}$	`BPRP PRI`
83839341 B	217.53558345727	−25.55056842979	$3.94^{+0.15}_{-0.23}$	2,046	$1.08^{+0.11}_{-0.12}$	$6,298^{+385}_{-322}$	`BPRP PRI`
98957720 B	180.99683654878	−28.32813097238	$9.80^{+0.03}_{-0.16}$	3,356	$0.45^{+0.01}_{-0.05}$	$3,317^{+19}_{-46}$	`BPRP PRI`
105850602 C	244.33420561134	16.42671038186	$11.26^{+0.06}_{-0.10}$	3,637	$0.23^{+0.01}_{-0.01}$	$3,213^{+10}_{-6}$	`inter BPRP`
105850602 D	244.33400811636	16.42673442250	$11.72^{+0.06}_{-0.10}$	3,553	$0.20^{+0.11}_{-0.07}$	$3,106^{+270}_{-295}$	
117644481 B	67.74861870851	−14.36826105677	$8.32^{+0.48}_{-0.43}$	5,179	$0.60^{+0.01}_{-0.05}$	$3,731^{+75}_{-77}$	`BPRP PRI`
135145585 B	185.41006070851	−41.19261307186	$9.81^{+0.14}_{-0.24}$	4,282	$0.45^{+0.01}_{-0.01}$	$3,280^{+83}_{-25}$	`BPRP`
139444326 B	80.73136663361	−21.95745238328	$9.92^{+0.41}_{-0.33}$	3,089	$0.37^{+0.04}_{-0.05}$	$3,442^{+73}_{-84}$	`inter BPRP`
142443425 B	146.55289564051	67.09725083384	$7.24^{+0.10}_{-0.09}$	389	$0.55^{+0.03}_{-0.01}$	$4,617^{+229}_{-508}$	`BPRP`
144164538 B	61.18284430216	−47.16584470949	$11.35^{+0.17}_{-0.41}$	354	$0.22^{+0.03}_{-0.01}$	$3,204^{+42}_{-25}$	`inter`
151628217 B	88.60524481432	−46.42448223827	$4.30^{+0.07}_{-0.10}$	7,075	$0.96^{+0.10}_{-0.10}$	$6,236^{+276}_{-248}$	`BPRP PRI`
152226055 B	312.48730424663	−33.27779249937	$6.70^{+0.32}_{-0.27}$	3,775	$0.74^{+0.01}_{-0.04}$	$4,562^{+124}_{-71}$	`BPRP PRI`
164781040 B	284.69989267282	46.37521416536	$5.49^{+0.34}_{-0.59}$	335	$0.80^{+0.22}_{-0.17}$	$5,434^{+782}_{-1004}$	
178367145 A	123.39224456462	−1.98278782520	$3.92^{+0.15}_{-0.12}$	1,265	$1.05^{+0.14}_{-0.11}$	$6,207^{+418}_{-323}$	`BPRP PRI`
197760286 B	331.50570859756	−37.28596009795	$8.69^{+0.07}_{-0.44}$	1,062	$0.54^{+0.02}_{-0.04}$	$3,711^{+28}_{-98}$	`BPRP PRI`
202712304 B	7.89840211300	50.95370147188	$10.94^{+0.39}_{-0.42}$	1,023	$0.32^{+0.03}_{-0.16}$	$3,017^{+40}_{-20}$	`BPRP PRI`
224327878 B	251.02883064726	30.00805300731	$11.01^{+0.06}_{-0.28}$	267	$0.25^{+0.03}_{-0.01}$	$3,239^{+43}_{-6}$	`inter EDR3 BPRP`
224327878 C	251.03000905102	30.01048010687	$10.99^{+0.06}_{-0.28}$	1,212	$0.32^{+0.01}_{-0.01}$	$3,055^{+51}_{-32}$	`BPRP PRI`

TABLE 3 Continued

CTOI	α (°)	δ (°)	M_G (mag)	*sep* (au)	*mass* ($M_\odot$)	T_{eff} (K)	Flags
230236827 B	261.53342682463	42.59471357813	$10.43^{+0.07}_{-0.30}$	354	$0.35^{+0.01}_{-0.01}$	$3,248^{+6}_{-6}$	BPRP PRI
238235254 A	119.80123285388	−49.97681348175	$-1.69^{+0.06}_{-0.12}$	6,822	$4.47^{+0.69}_{-0.36}$	$13,518^{+1839}_{-1222}$	BPRP PRI
238920872 B	94.29032954304	−52.34601641705	$11.82^{+0.13}_{-0.13}$	4,813	$0.12^{+0.13}_{-0.01}$	$2,823^{+58}_{-16}$	BPRP
253040591 B	159.25714983803	42.12868405630	$13.01^{+0.17}_{-0.17}$	640			WD BPRP
257605131 B	62.95486583450	−37.94500665138	$8.33^{+0.07}_{-0.16}$	4,669	$0.60^{+0.01}_{-0.01}$	$3,728^{+15}_{-69}$	BPRP PRI
259376845 B	68.46856153261	−51.25247980639	$5.28^{+0.17}_{-0.13}$	1,177	$0.87^{+0.06}_{-0.05}$	$5,457^{+283}_{-231}$	BPRP PRI
282502866 B	90.09431406761	1.80160968503	$10.41^{+0.13}_{-0.08}$	3,375	$0.29^{+0.06}_{-0.06}$	$3,066^{+47}_{-24}$	BPRP PRI
288240183 B	224.78438383542	83.34266967111	$4.58^{+0.16}_{-0.17}$	9,044	$0.93^{+0.09}_{-0.07}$	$5,866^{+305}_{-286}$	BPRP PRI
288240183 C	224.78626346820	83.34221655772	$9.88^{+0.25}_{-0.25}$	8,771	$0.35^{+0.15}_{-0.15}$	$3,478^{+348}_{-288}$	
290596728 B	306.89728308250	−40.36459462135	$7.74^{+0.25}_{-0.20}$	818	$0.60^{+0.04}_{-0.01}$	$4,031^{+80}_{-66}$	BPRP PRI
300116105 B	92.47405292459	−39.73999660669	$9.19^{+0.11}_{-0.10}$	738	$0.46^{+0.01}_{-0.01}$	$3,623^{+33}_{-42}$	inter BPRP
308301091 B	267.86777900177	24.81212544714	$10.32^{+0.18}_{-0.16}$	715	$0.31^{+0.14}_{-0.11}$	$3,398^{+326}_{-280}$	
312091232 B	140.31670670796	6.65786362756	$10.00^{+0.13}_{-0.14}$	2,271	$0.37^{+0.02}_{-0.01}$	$3,422^{+34}_{-27}$	inter EDR3 BPRP
326092637 B	15.37238815490	−24.93391132753	$11.59^{+0.10}_{-0.25}$	8,137	$0.21^{+0.02}_{-0.01}$	$3,168^{+37}_{-16}$	inter BPRP
341411516 B	119.93640614165	−59.26953097644	$13.48^{+0.02}_{-0.12}$	4,162			WD BPRP
345324572 A	355.48235281306	59.88525830586	$5.20^{+0.19}_{-0.15}$	1,616	$0.90^{+0.06}_{-0.06}$	$5,475^{+239}_{-211}$	BPRP PRI
349793830 B	143.44650893948	24.26182131498	$12.70^{+0.03}_{-0.08}$	2,308	$0.16^{+0.01}_{-0.01}$	$2,862^{+5}_{-16}$	BPRP
352915304 B	313.79523211150	62.77508729271	$11.92^{+0.02}_{-0.13}$	427	$0.19^{+0.01}_{-0.01}$	$3,116^{+21}_{-3}$	inter BPRP
369376388 B	59.85169681654	−36.47623340570	$11.97^{+0.44}_{-0.34}$	157	$0.17^{+0.08}_{-0.06}$	$3,053^{+249}_{-293}$	
369376388 C	59.85740294934	−36.47089495211	$11.62^{+0.44}_{-0.34}$	2,292			WD BPRP
372913337 B	119.48675278787	−60.84268804035	$4.07^{+0.11}_{-0.24}$	5,924	$1.02^{+0.11}_{-0.10}$	$6,213^{+333}_{-342}$	BPRP PRI
374352402 B	303.50138009888	−69.43373843927	$6.58^{+0.29}_{-0.39}$	2,025	$0.70^{+0.06}_{-0.05}$	$4,752^{+285}_{-289}$	BPRP
374732772 B	242.12692516072	−38.47303765313	$6.83^{+0.49}_{-0.43}$	775	$0.69^{+0.04}_{-0.04}$	$4,457^{+259}_{-227}$	inter BPRP PRI
394721720 B	20.29820671156	−85.59341646735	$10.52^{+0.15}_{-0.15}$	4,040	$0.30^{+0.02}_{-0.02}$	$3,322^{+28}_{-28}$	inter BPRP
399913539 B	287.26229580166	48.84559355879	$10.31^{+0.23}_{-0.31}$	1,622	$0.33^{+0.04}_{-0.03}$	$3,361^{+61}_{-43}$	inter BPRP
453455638 B	151.96566880705	−76.28161439253	$9.51^{+0.25}_{-0.17}$	1,907	$0.48^{+0.02}_{-0.03}$	$3,370^{+190}_{-38}$	BPRP PRI
460950389 B	159.14432531677	−64.81206485569	$14.31^{+0.15}_{-0.15}$	8,128	$0.10^{+0.01}_{-0.01}$	$2,876^{+23}_{-182}$	inter BPRP
467785319 B	62.74680893665	34.15885055036	$10.77^{+0.14}_{-0.14}$	493	$0.28^{+0.02}_{-0.02}$	$3,274^{+26}_{-25}$	inter BPRP
738065944 B	98.61713426810	−41.14765885257	$5.71^{+0.32}_{-0.21}$	857	$0.78^{+0.22}_{-0.18}$	$5,311^{+813}_{-1075}$	
901674675 B	165.50033761990	−25.69109105001	$3.99^{+0.23}_{-0.10}$	1,127	$1.03^{+0.12}_{-0.12}$	$6,220^{+393}_{-318}$	BPRP PRI

Note: The flags for all companions, as defined in the text, are listed in the last column of this table.

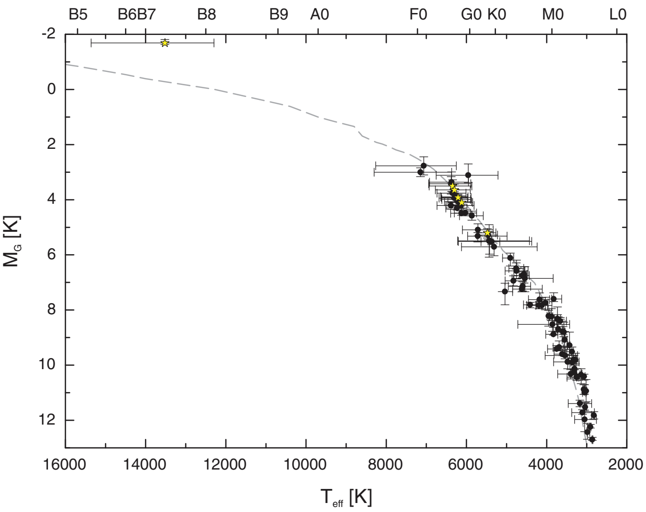

FIGURE 4 This T_{eff}-M_{G} diagram shows all detected companions, whose effective temperatures are either listed in the SHC or for which Apsis-Priam temperature estimates are available. Companions, which are the primary components of their stellar systems, are illustrated as yellow star symbols. The main sequence is plotted as dashed gray line for comparison

of all detected companions except for CTOI 253040591 B, CTOI 341411516 B, CTOI 369376388 C, TOI 2092 B, and TOI 2127 B. We summarize the photometric properties of these companions in Table 4. The companions are all several magnitudes fainter than the associated (C)TOIs, but appear bluer than their primaries. Furthermore, the temperatures of these companions, derived from their absolute G-band magnitudes, adopting that they are main-sequence stars, is about 2,800–7,800 K lower than the temperatures, obtained from their colors, which are listed in Table 4.

In Figure 5, we plot these companions together with the other components of their stellar systems, in a T_{eff}-M_{G} diagram. For comparison, we show in this diagram the main sequence from Pecaut & Mamajek (2013), as well as evolutionary mass tracks of DA white dwarfs from the white dwarf models of Holberg & Bergeron (2006), Kowalski & Saumon (2006), Tremblay et al. (2011), and Bergeron et al. (2011). While the brighter primary components of these systems as well as the secondary CTOI 369376388 B are all main-sequence stars the five faint companions are clearly located below the main sequence and their Gaia photometry is well consistent with that expected for white dwarfs, except for TOI 2127 B, which is discussed in more detail below.

As shown in Figure 6, due to their wider angular separations ($\rho \gtrsim 8.8$ arcsec) the faint companions CTOI 253040591 B, CTOI 341411516 B, and CTOI 369376388 C are all detected next to their primaries in all sky survey images, taken in the optical spectral range, while they remain invisible in the near-infrared J-band images of the Two Micron All Sky Survey (2MASS). If these three companions would be low-mass main-sequence stars their absolute G-band magnitudes correspond to masses in the range between 0.12 and 0.2 $M_{\odot}$. Such low-mass companions would exhibit apparent J-band magnitudes between 14.0 and 16.2 mag (extinction is taken into account, adopting $A_J/A_G = 0.34$, as derived by Mugrauer 2019). As the 2MASS J-band images exhibit $SNR = 10$ detection limits between 16.4 and 16.6 mag, the companions should easily be detectable in these images, which is however not the case. Hence, the companions exhibit an intrinsic faintness in both the optical and near infrared spectral range that clearly rules out that they are low-mass main-sequence stars. Therefore, we conclude that these stars are all white dwarf companions of the associated (C)TOIs, which is indicated with the `WD` flag in Table 3.

As illustrated in the T_{eff}-M_{G} diagram in Figure 5, TOI 2127 B is located in the range between the main sequence and the white dwarf tracks slightly closer to these tracks than to the main sequence. Hence, from its Gaia photometry alone the classification of the nature of this companion remains uncertain. However, TOI 2127 (alias HAT-P-18) was also observed in the near infrared (F139M) with the Wide Field Camera 3 (WFC3), aboard of the Hubble Space Telescope (HST). Two images of the star were taken on February 11, 2016, and on January 12, 2017, each with an integration time of 29.7 s. Beside the exoplanet host star also its faint companion TOI 2127 B is detected in the HST images on average at $\rho = 2.667 \pm 0.006$ arcsec & $PA = 186.2 \pm 0.3°$, very well consistent with the relative

TABLE 4 The photometry of the five white dwarf companions, detected in this survey

Companion	$\Delta(B_P - R_P)$ (mag)	ΔG (mag)	$(B_P - R_P)$ (mag)	$(B_P - R_P)_0$ (mag)	T_{eff} (K)
CTOI 253040591 B	-0.2954 ± 0.0454	8.6180 ± 0.0042	0.5392 ± 0.3322	$0.3672^{+0.3378}_{-0.3555}$	7263^{+1932}_{-1141}
CTOI 341411516 B	-0.3460 ± 0.0714	8.6006 ± 0.0053	0.4841 ± 0.0698	$0.4724^{+0.0704}_{-0.0859}$	6879^{+309}_{-230}
CTOI 369376388 C	-1.3829 ± 0.0120	5.1889 ± 0.0040	0.1757 ± 0.0088	$-0.1438^{+0.1745}_{-0.1141}$	10916^{+1038}_{-1841}
TOI 2092 B	-0.2398 ± 0.2533	8.3105 ± 0.0096	0.6278 ± 0.2532	$0.5768^{+0.2548}_{-0.2599}$	6542^{+974}_{-820}
TOI 2127 B	-0.3113 ± 0.1537	6.5909 ± 0.0064	0.9283 ± 0.1537	$0.8203^{+0.1637}_{-0.1594}$	5785^{+485}_{-513}

Note: For each companion we list the color difference $\Delta(B_P - R_P)$, and the G-band magnitude difference ΔG to the associated (C)TOI, its apparent $(B_P - R_P)$ color, as well as its derived intrinsic color $(B_P - R_P)_0$, and effective temperature T_{eff}.

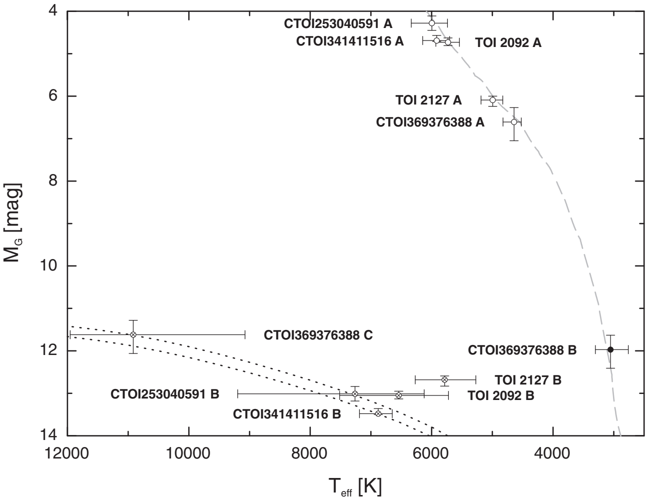

FIGURE 5 T_{eff}-M_{G} diagram of the stellar systems with white dwarf components, detected in this survey. The main sequence is plotted as gray dashed line and the evolutionary mass tracks of DA white dwarfs with masses of 0.5 and 0.6 $M_{\odot}$ as black dotted lines, respectively. The primaries of the systems are shown as white circles, main-sequence companions as black, and white dwarf companions as white crossed circles, respectively

Gaia EDR3 astrometry of the companion, as listed in Table 2. The first epoch WFC3 image of TOI 2127 is shown in Figure 7.

We have used aperture photometry to determine the magnitude difference between the companion and the exoplanet host star in both WFC3 images and obtained ΔF139M $= 8.01 \pm 0.09$ mag. The exoplanet host star is listed in the SHC as a main-sequence star with a mass of $0.78^{+0.02}_{-0.04} M_{\odot}$. If its companion would be a low-mass main-sequence star as well, its absolute G-band magnitude, listed in Table 3, corresponds to a mass of $0.15 \pm 0.01 M_{\odot}$, following the M_{G}-mass relation from Pecaut & Mamajek (2013). According to the Dartmouth Stellar Evolution Database (Dotter et al. 2008), for such a low-mass stellar companion we would expect a magnitude difference to HAT-P-18 of $\Delta F139\mathrm{M} = 4.7^{+0.2}_{-0.3}$ mag at the age of the exoplanet host star of about 12 Gyr (Hartman et al. 2011). However, the companion is significantly fainter (by about 3.3 mag) in the near infrared than expected for a low-mass main-sequence star. Therefore, from its Gaia and HST photometry we conclude that TOI 2127 B is a white dwarf companion of the exoplanet host star. Follow-up spectroscopic observations are needed to further constrain its properties, as well as those of all the other degenerated companions, detected in this survey.

The histograms of the properties of all companions, presented here, are illustrated in Figure 8. The companions exhibit angular separations to the (C)TOIs, in the range between about 0.8 and 63 arcsec, which corresponds to projected separations of 117 up to 9,463 au. According to the underlying cumulative distribution function, the frequency of the companions is the highest and constant up to about 500 au while it continually decreases for larger projected separations. Half of all companions exhibit projected separations of less than 1,300 au. In total, seven stellar systems (six binaries and one hierarchical triple) are detected with projected separations below 200 au, namely: TOI 2009 AB, TOI 2072 AB, TOI 2183 AB, TOI 2299 AB, TOI 2384 AB, TOI 2422 AB, and CTOI 369376388 AB+C(WD), i.e. these systems are the most challenging environments for planet formation, identified in this study.

The masses of the companions range between about 0.09 $M_{\odot}$ and 4.5 $M_{\odot}$ (average mass is ~0.6 $M_{\odot}$). The highest companion frequency is found in the cumulative distribution function in the mass range between 0.15 and 0.6 $M_{\odot}$, which corresponds beside detected white dwarf companions mainly to mid M to late K dwarfs, according to the relation between mass and spectral type (SpT), described by Pecaut & Mamajek (2013). For higher masses, the companion frequency is lower but constant up to about 1.2 $M_{\odot}$ from where it significantly decreases toward higher masses. This peak in the companion population is also detected in the distribution of their effective temperatures, which exhibits the highest frequency of companions in the temperature range between 3,000 and 4,000 K. In this distribution also, a second but fainter pile-up of companions is prominent, which is located between about 6,000 and 6,500 K and corresponds to late to mid F type stars, according to the T_{eff}-SpT relation from Pecaut & Mamajek (2013).

As shown in the separation-mass diagram in Figure 9, among all 119 companions, presented here, 6 are the primary, 106 the secondary, 6 are the tertiary, and one is the quaternary component of their stellar systems.

In order to characterize the detection limit, reached in this survey, we plot the magnitude differences of all detected companions over their angular separations to the associated (C)TOIs, as shown in Figure 10.

For comparison, we show the Gaia DR2 detection limit, determined by Mugrauer & Michel (2020) among (C)TOIs, which are brighter than $G = 12.8$ mag (about 88% of the targets with detected companions of the survey, presented here). Companions with angular separations larger than about 1 arcsec are detectable around bright (C)TOIs while closer companions slightly below this separation limit with magnitude differences up to about 3 mag can be detected by Gaia around fainter targets. The companions, identified in this survey with astrometric solutions listed also in the Gaia DR2, all agree with the determined Gaia detection limit. In contrast, four companions detected in this survey around bright (C)TOIs exceed this specific limit. However, the astrometric solutions of these companions are listed only in the Gaia EDR3. In addition, all of the

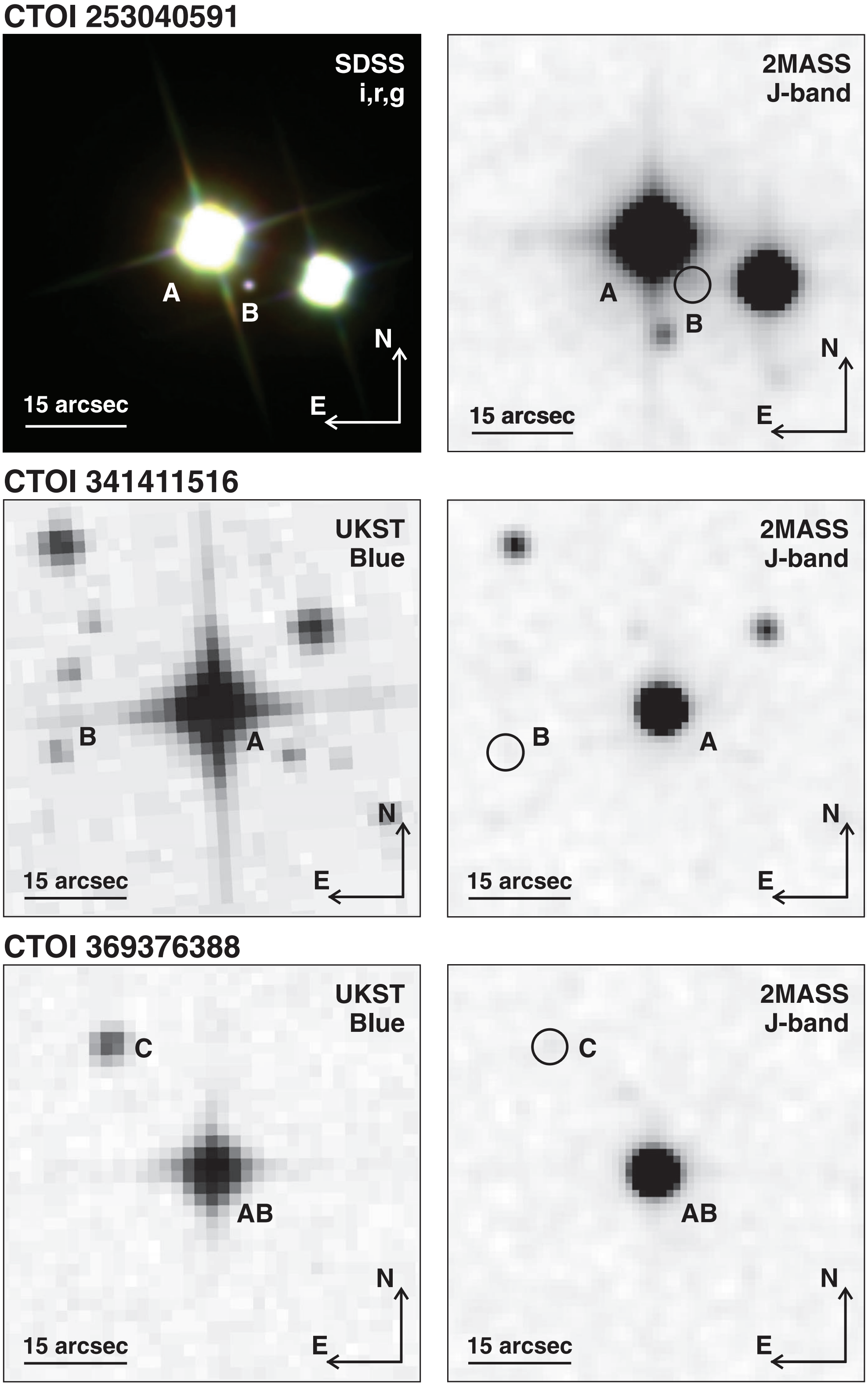

FIGURE 6 A color(RGB)-composite image of the white dwarf CTOI 253040591 B, created from imaging data, taken in the course of the Sloan Digital Sky Survey (SDSS) in the i-, r-, and g-band together with images of the white dwarf companions CTOI 341411516 B, and CTOI 369376388 C, taken with the UK Schmidt Telescope (UKST) in the filter GG395. 2MASS J-band images of the CTOIs are shown for comparison with the expected position of the companions, indicated with black circles. While the companions are all well detected in the optical spectral range they remain invisible in the 2MASS images, consistent with the photometric properties expected for the companions in the case that they are white dwarfs

companions, whose astrometric solutions are listed only in this Gaia data release have angular separations from the associated (C)TOIs, which are smaller than about 8 arcsec. Both indicate that the Gaia EDR3 has a higher sensitivity to close companions compared to its precursor.

The expected magnitude differences between the targets of this survey and low-mass main-sequence companions (indicated with gray dashed lines in Figure 10) are estimated with the expected absolute G-band magnitudes of these stars, as listed by Pecaut & Mamajek (2013), and

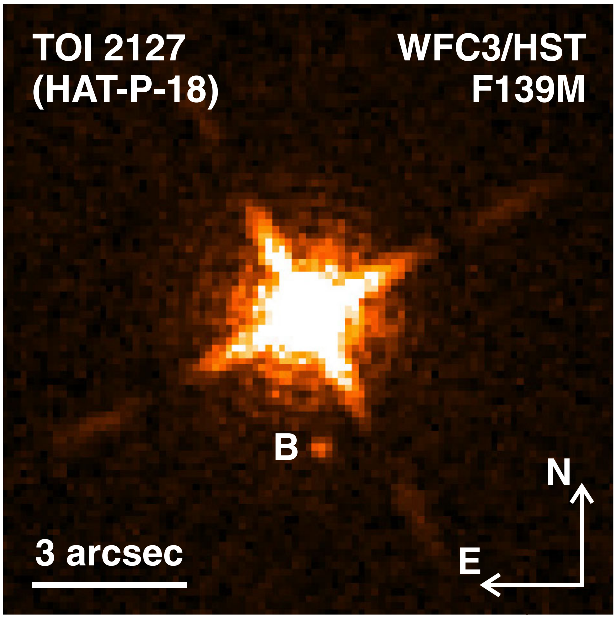

FIGURE 7 TOI 2127 (alias HAT-P-18) observed on February 11, 2016 in the near infrared (F139M) with the WFC3 camera, aboard of the Hubble Space Telescope. The faint companion TOI 2127 B is well detected in the image south of the exoplanet host star

the average absolute G-band magnitude of our targets ($M_G = 4.5$ mag). As shown in Figure 10, a magnitude difference of about 3.4 mag is reached at an angular separation of about 1.4 arcsec around the targets of this survey. This allows the detection of companions with masses down to about 0.6 $M_\odot$ (average mass of all detected companions) which are separated from the (C)TOIs by more than 340 au. Furthermore, companions with masses down to about 0.1 $M_\odot$ are detectable beyond 6 arcsec, which corresponds to a projected separation of 1,440 au at the average target distance of 240 pc.

4 | SUMMARY AND OUTLOOK

The goal of the survey, whose latest results are presented here, is the detection and characterization of stellar companions of (C)TOIs, i.e. of potential exoplanet host stars. In this paper, we have explored the multiplicity of 585 (C)TOIs, which were announced in the (C)TOI Release of the ExoFOP-TESS between the end of May and the beginning of December 2020.

In contrast to Mugrauer & Michel (2020), who explored the Gaia DR2 to search for companions around (C)TOIs, the continuation of this survey, presented here, is based on Gaia EDR3 astro- and photometry. We have used the target sample as well as the detected companions to characterize the differences between both Gaia data releases regarding their sensitivity and the accuracy of their astrometric solutions. Within the applied search radius around the targets in total about 36,100 sources with accurate astrometric solutions were identified in the Gaia EDR3 while only about 34,000 such objects were found in the same regions on the sky in the Gaia DR2. In addition, among all 119 companions, detected in this survey, 12 have astrometric solutions only listed in the Gaia EDR3 (indicated with the EDR3 flag in Table 3) and all of these companions are located within 8 arcsec around the associated (C)TOIs. Therefore, we conclude that the Gaia EDR3 contains about 10% more sources with accurate astrometric solutions and is more sensitive in particular for close companions at angular separations below about 10 arcsec compared to its precursor. In addition, the astrometric solutions of the targets and their companions in the Gaia EDR3 exhibit uncertainties in their astrometric position, parallax, and proper motion, which are smaller by factors of about 0.6, 0.6, and 0.4, respectively, compared to the Gaia DR2. The larger number of detected sources, the higher sensitivity in particular for close companions, as well as the more accurate astrometry of the Gaia EDR3 compared to its precursor, found in this study, all agree well with the general characteristics of both Gaia data releases, as described by Gaia Collaboration et al. (2018), and Gaia Collaboration et al. (2020).

In total, we have detected companions around 113 of the 585 targets, whose multiplicity was studied here. Hence, the multiplicity rate of the investigated (C)TOIs is at least about $19 \pm 2\%$, which is consistent with the multiplicity rate of (C)TOIs, reported by Mugrauer & Michel (2020).

Beside 107 binaries also 5 hierarchical triple star systems and one quadruple system were detected, in which either the (C)TOI exhibits a close and a wide companion or a close binary companion instead, which is located at a wider angular separation. As it is expected for the components of gravitationally bound stellar systems, the (C)TOIs and the detected companions are equidistant and share a common proper motion, as proven with their accurate Gaia EDR3 parallaxes and proper motions. In particular, the direct proof of equidistance of the individual components of the stellar systems, as done in this survey by comparing their parallaxes, was not feasible in earlier multiplicity surveys before the release of the accurate Gaia data because in particular for the majority of the faint companions their parallaxes could not be measured by the ESA-Hipparcos mission (Perryman et al. 1997).

However, 35 companions, identified in this survey, were already listed in the WDS, either as co-moving companions or as companion-candidates of the (C)TOIs, which still needed confirmation of their companionship, eventually yielded by this survey. Although the WDS is currently the most complete available catalog of multiple

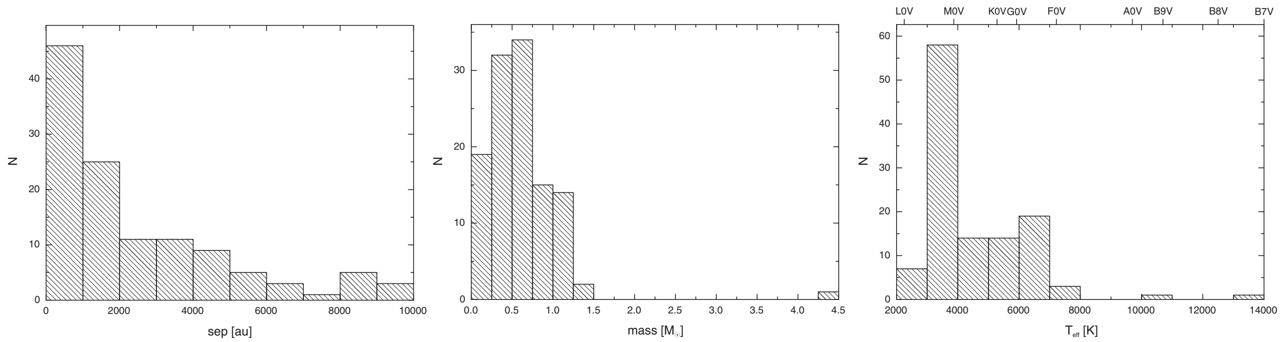

FIGURE 8 The histograms of the properties of the companions, detected in this survey

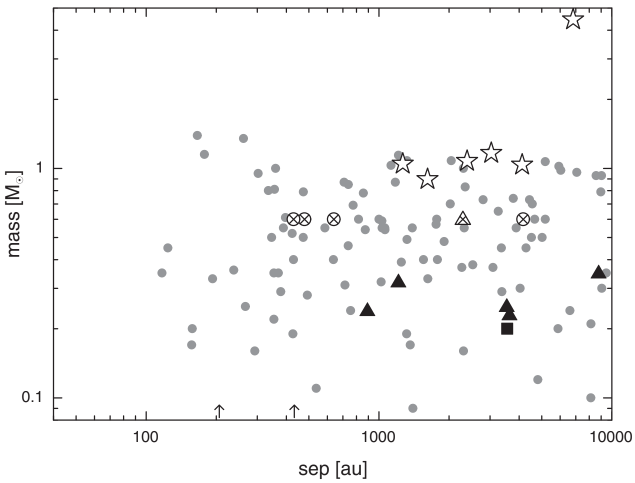

FIGURE 9 The separation-mass diagram of the companions, detected in this survey. Companions, which are the primary components of their stellar systems, are plotted as star symbols, those which are secondaries as circles, tertiary components as triangles, and quaternary components as squares, respectively. Detected white dwarf companions, for which a mass of 0.6 $M_\odot$ is adopted, are plotted with white crossed symbols. The separations of the two companions TOI 2001 B, and TOI 2115 B, for which no masses could be determined, are indicated with black arrows

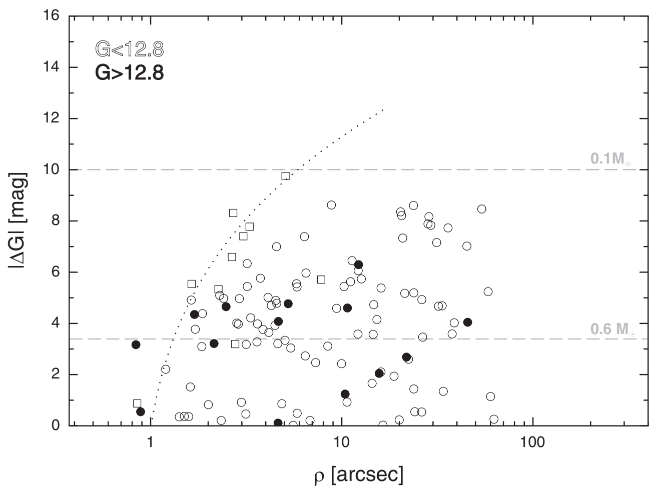

FIGURE 10 The magnitude differences of all detected companions plotted versus their angular separations to the associated (C)TOIs. The Gaia detection limit, found by Mugrauer & Michel (2020), is shown as dotted line for comparison. The expected average magnitude difference for companions with 0.1 or 0.6 $M_\odot$ is drawn as gray dashed horizontal lines. Companions of (C)TIOs brighter and fainter than G = 12.8 mag are plotted as open circles and filled black circles, respectively. Companions, whose astrometric solutions are only listed in the Gaia EDR3, are shown as open boxes

star systems, which contains relative astrometric measurements of multiple systems spanning a period of more than 300 years, in this study 84 (i.e. 70% of all) companions were detected, which are not listed in the WDS, indicated with the ⋆ flag in Table 2. This demonstrates the great potential of the ESA-Gaia mission for multiplicity studies of stars, in particular, for the detection of wide companions, as it is illustrated with the derived detection limit of this survey, shown in Figure 10. On average, all stellar companions with masses down to about 0.1 $M_\odot$ are detectable in this study around the targets beyond about 6 arcsec (or 1,440 au of projected separation) and approximately half of all detected companions exhibit such separations. In total, companions are identified with projected separations between about 120 and 9,500 au and the frequency of companions is constant up to about 500 au and continually decreases for larger projected separations. The companions, detected in this survey, exhibit masses in the range between about 0.09 $M_\odot$ and 4.5 $M_\odot$ and are most frequently found in the mass range between 0.15 and 0.6 $M_\odot$. Beside low-mass main-sequence stars (mainly early to mid M dwarfs) also 5 white dwarfs could be identified as co-moving companions of the (C)TOIs, whose true nature was revealed in this survey, using their accurate astro- and photometric properties.

For 99 (i.e. about 83% of all) companions, presented here, significant ($sig\text{-}\mu_{\rm rel} \geq 3$) differential proper motions $\mu_{\rm rel}$ relative to the associated (C)TOIs were detected. We derived the escape velocities $\mu_{\rm esc}$ of all these companions using the approximation, described in Mugrauer (2019).

TABLE 5 List of all detected companions (sorted by their identifier), whose differential proper motions μ_{rel} relative to the (C)TOIs significantly exceed the expected escape velocities μ_{esc}

Companion	μ_{rel} (mas year^{-1})	μ_{esc} (mas year^{-1})	
TOI 1946 B	5.65 ± 0.22	2.09 ± 0.07	
TOI 1966 B	1.06 ± 0.04	0.52 ± 0.02	
TOI 2006 B	0.68 ± 0.02	0.54 ± 0.03	
TOI 2050 B	4.93 ± 0.04	2.51 ± 0.06	
TOI 2218 A	2.42 ± 0.05	0.74 ± 0.04	
TOI 2239 B	0.58 ± 0.02	0.30 ± 0.02	
TOI 2281 B	1.26 ± 0.02	0.96 ± 0.05	
TOI 2325 B	2.59 ± 0.05	1.73 ± 0.01	
TOI 2358 B	1.75 ± 0.16	0.58 ± 0.03	
TOI 2409 B	3.11 ± 0.03	0.87 ± 0.02	
TOI 2417 B	3.23 ± 0.03	2.13 ± 0.09	
CTOI 35703676 B	3.71 ± 0.10	0.50 ± 0.03	
CTOI 135145585 B	4.19 ± 0.09	0.42 ± 0.02	
CTOI 151628217 B	1.35 ± 0.02	0.31 ± 0.02	
CTOI 197760286 B	5.51 ± 0.14	1.92 ± 0.13	
CTOI 230236827 B	6.56 ± 0.05	5.68 ± 0.02	
CTOI 288240183 B	5.46 ± 0.51	0.98 ± 0.10	⋆⋆⋆
CTOI 288240183 C	3.77 ± 0.53	0.87 ± 0.05	⋆⋆⋆
CTOI 300116105 B	1.95 ± 0.10	1.24 ± 0.05	

Note: Companions, which are already known to be members of hierarchical triple star systems, are indicated with ⋆⋆⋆.

The differential proper motion of most of these companions is consistent with orbital motion. In contrast for 19 companions, their differential proper motions significantly exceed the expected escape velocities, indicating an increased degree of multiplicity, as discussed in Mugrauer (2019). Two of these companions are located in an already confirmed hierarchical triple star system. Follow-up high contrast imaging observations are needed to further explore the multiplicity status of all these particular systems and their companions, which are summarized in Table 5.

The survey, whose latest results are presented here, is an ongoing project and its target list is steadily growing due to the continuing analysis of photometric data, collected by the TESS mission. The multiplicity of all these newly revealed (C)TOIs will be explored in the course of this survey and detected companions and their determined properties will be reported regularly in this journal and will also be made available online in the `VizieR` database (Ochsenbein et al. 2000),[5] and at the Webpage of the survey.[6] The results of this survey combined with those of high-contrast imaging observations of the (C)TOIs, which can detect close companions with projected separations down to only a few au, will complete our knowledge of the multiplicity of all these potential exoplanet host stars.

ACKNOWLEDGMENTS

We made use of data from:

1. the `Simbad` and `VizieR` databases operated at CDS in Strasbourg, France.
2. the European Space Agency (ESA) mission Gaia (https://www.cosmos.esa.int/gaia), processed by the Gaia Data Processing and Analysis Consortium (DPAC, https://www.cosmos.esa.int/web/gaia/dpac/consortium). Funding for the DPAC has been provided by national institutions, in particular the institutions participating in the Gaia Multilateral Agreement.
3. the `Exoplanet Follow-up Observing Program` website, which is operated by the California Institute of Technology, under contract with the National Aeronautics and Space Administration under the Exoplanet Exploration Program.
4. the Two Micron All Sky Survey, which is a joint project of the University of Massachusetts and the Infrared Processing and Analysis Center/California Institute of Technology, funded by the National Aeronautics and Space Administration and the National Science Foundation.
5. the Digitized Sky Surveys, which were produced at the Space Telescope Science Institute (STScI) under U.S. Government grant NAG W-2166. The images of these surveys, used here, were taken with the UK Schmidt Telescope, which was operated by the Royal Observatory Edinburgh, with funding from the UK Science and Engineering Research Council (later the UK Particle Physics and Astronomy Research Council), until 1988 June and thereafter by the Anglo-Australian Observatory. Supplemental funding for sky-survey work at the STScI is provided by the European Southern Observatory.
6. the Sloan Digital Sky Survey (SDSS) which has been provided by the Alfred P. Sloan Foundation, the Participating Institutions, the National Aeronautics and Space Administration, the National Science Foundation, the U.S. Department of Energy, the Japanese Monbukagakusho, and the Max Planck Society. The SDSS

[5]Online available at: https://vizier.u-strasbg.fr/viz-bin/VizieR
[6]Online available at: https://www.astro.uni-jena.de/Users/markus/Multiplicity_of_(C)TOIs.html

Web site is http://www.sdss.org/. The SDSS is managed by the Astrophysical Research Consortium (ARC) for the Participating Institutions. The Participating Institutions are The University of Chicago, Fermilab, the Institute for Advanced Study, the Japan Participation Group, The Johns Hopkins University, Los Alamos National Laboratory, the Max-Planck-Institute for Astronomy (MPIA), the Max-Planck-Institute for Astrophysics (MPA), New Mexico State University, University of Pittsburgh, Princeton University, the United States Naval Observatory, and the University of Washington.

7. the Pan-STARRS1 surveys, which were made possible through contributions by the Institute for Astronomy, the University of Hawaii, the Pan-STARRS Project Office, the Max-Planck Society and its participating institutes, the Max Planck Institute for Astronomy, Heidelberg and the Max Planck Institute for Extraterrestrial Physics, Garching, The Johns Hopkins University, Durham University, the University of Edinburgh, the Queen's University Belfast, the Harvard-Smithsonian Center for Astrophysics, the Las Cumbres Observatory Global Telescope Network Incorporated, the National Central University of Taiwan, the Space Telescope Science Institute, and the National Aeronautics and Space Administration under Grant No. NNX08AR22G issued through the Planetary Science Division of the NASA Science Mission Directorate, the National Science Foundation Grant No. AST-1238877, the University of Maryland, Eotvos Lorand University (ELTE), and the Los Alamos National Laboratory. The Pan-STARRS1 Surveys are archived at the Space Telescope Science Institute (STScI) and can be accessed through MAST, the Mikulski Archive for Space Telescopes. Additional support for the Pan-STARRS1 public science archive is provided by the Gordon and Betty Moore Foundation.

Open Access funding enabled and organized by Projekt DEAL.

REFERENCES

Anders, F., Khalatyan, A., Chiappini, C., et al. 2019, *A&A*, *628*, A94.
Andrae, R., Fouesneau, M., Creevey, O., et al. 2018, *A&A*, *616*, A8.
Bergeron, P., Wesemael, F., Dufour, P., et al. 2011, *ApJ*, *737*(1), 28.
Dotter, A., Chaboyer, B., Jevremović, D., Kostov, V., Baron, E., & Ferguson, J. W. 2008, *ApJS*, *178*(1), 89.
Gaia Collaboration, Brown, A. G. A., Vallenari, A., et al. 2018, *A&A*, *616*, A1.
Gaia Collaboration, Brown, A. G. A., Vallenari, A., Prusti, T., de Bruijne, J. H. J., Babusiaux, C., & Biermann, M. 2020, December, *arXiv e-prints*, arXiv:2012.01533.
Hartman, J. D., Bakos, G. Á., Sato, B., et al. 2011, *ApJ*, *726*(1), 52.
Holberg, J. B., & Bergeron, P. 2006, *AJ*, *132*, 1221.
Kowalski, P. M., & Saumon, D. 2006, *ApJL*, *651*, L137.
Lindegren, L., Klioner, S. A., Hernández, J. et al. 2020, December, *arXiv e-prints*, arXiv:2012.03380.
Martin, D. V., El-Badry, K., Kunovac Hodžić, V. et al. 2021, January, *arXiv e-prints*, arXiv:2101.02707.
Mason, B. D., Wycoff, G. L., Hartkopf, W. I., Douglass, G. G., & Worley, C. E. 2001, *AJ*, *122*(6), 3466.
Michel, K. U., & Mugrauer, M. 2021, February, *arXiv e-prints*, arXiv:2102.04385.
Mugrauer, M. 2019, *MNRAS*, *490*(4), 5088.
Mugrauer, M., & Michel, K.-U. 2020, *Astron. Nachr.*, *341*(10), 996.
Newton, E. R., Mann, A. W., Kraus, A. L., et al. 2021, *AJ*, *161*(2), 65.
Ochsenbein, F., Bauer, P., & Marcout, J. 2000, *A&AS*, *143*, 23.
Pecaut, M. J., & Mamajek, E. E. 2013, *ApJS*, *208*, 9.
Perryman, M. A. C., Lindegren, L., Kovalevsky, J., et al. 1997, *A&A*, *500*, 501.
Queiroz, A. B. A., Anders, F., Chiappini, C., et al. 2020, *A&A*, *638*, A76.
Ricker, G. R., Winn, J. N., Vanderspek, R., et al. 2015, *JATIS*, *1*, 014003.
Rodriguez, J. E., Quinn, S. N., Zhou, G. et al. 2021, *arXiv e-prints*, arXiv:2101.01726.
Tofflemire, B. M., Rizzuto, A. C., Newton, E. R. et al. 2021, February, *arXiv e-prints*, arXiv:2102.06066.
Tremblay, P.-E., Bergeron, P., & Gianninas, A. 2011, *ApJ*, *730*, 128.

AUTHOR BIOGRAPHY

Markus Mugrauer obtained his Diploma at the Technical University Munich and his PhD at the Friedrich-Schiller-University Jena. He works as staff astronomer at the University Observatory Jena.

How to cite this article: Mugrauer M, Michel K-U. Gaia search for stellar companions of TESS Objects of Interest II. *Astron. Nachr*. 2021;1–25. https://doi.org/10.1002/asna.202113972